Czech Technical University in Prague
Faculty of Nuclear Sciences and Physical Engineering

Department of Nuclear Reactors
Field of study: Nuclear Engineering

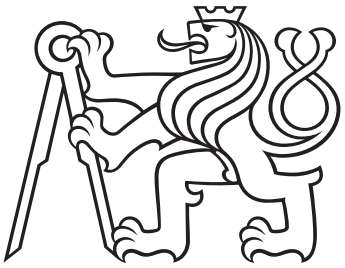

Spatial effects in reactivity measurements in subcritical states of research reactors

Prostorové vlivy při měření reaktivity v podkritických stavech výzkumných reaktorů

DIPLOMA THESIS

Author: Bc. Petr Kladiva
Supervisor: Ing. Tomáš Bíly, Ph.D.
Year: 2022

ČESKÉ
VYSOKÉ UČENÍ
TECHNICKÉ V PRAZE

Fakulta jaderná
a fyzikálně
inženýrská

Břehová 7 115 19 Praha 1

Katedra jaderných reaktorů

Akademický rok: 2022/2023

ZADÁNÍ DIPLOMOVÉ PRÁCE

Student:	**Bc. Petr Kladiva**
Studijní program:	Jaderné inženýrství
Specializace:	Jaderné reaktory
Název práce česky:	**Prostorové vlivy při měření reaktivity v podkritických stavech výzkumných reaktorů**
Název práce anglicky:	Spatial effects in reactivity measurements in subcritical states of research reactors
Jazyk práce:	angličtina

Pokyny pro vypracování:

1. Proveďte rešerši metod měření podkritičnosti na výzkumných reaktorech s důrazem na vliv místa měření.
2. Popište možnosti realizace výše popsaných metod na reaktoru TRIGA-MARK v Pavii a na reaktoru VR-1 na ČVUT v Praze včetně dostupného experimentálního vybavení. Diskutujte relevantní aspekty a případná omezení jejich realizace.
3. Vyberte jednu z uvedených metod. Navrhněte, proveďte a vyhodnoťte experiment věnovaný stanovení reaktivity v podkritickém stavu na reaktoru TRIGA v Pavii. Zpracujte korekce na prostorové efekty pomocí vhodného výpočetního nástroje.
4. Diskutujte možnosti stanovení reaktivity v podkritickém stavu reaktoru s uvažováním prostorových efektů s využitím provozních dat reaktoru VR-1. Demonstrujte zjištění na provozních datech naměřených na reaktoru VR-1 nebo datech poskytnutých vedoucím.

Doporučená literatura:

[1] IAEA. History, Development and Future of TRIGA Research Reactors. Vídeň:Technical Reports Series #482. 2016. ISBN 978-9201020161

[2] BLAISE P., MELLIER F., a P. FOUGERAS. Application of the Modified Source Multiplication (MSM) technique to subcritical reactivity worth measurements in thermal and fast reactor systems, In.: IEEE 2009 1st International Conference on Advancements in Nuclear Instrumentation, Measurement Methods and their Applications (ANIMMA). Marseille: IEEE. 2009, s. 1-9. ISBN: 978-142445208-8

[3] LECOUEY J.-L. a kol. Monte Carlo MSM correction factors for control rod worth estimates in subcritical and near-critical fast neutron reactors.EPJ Nuclear Sciences and Technologies. 2015, č. 1, s. 2.1 -2.9. ISSN 2491-9292

[4] RATAJ, J., HUML O., a L. SKLENKA. Experimentální neutronová a reaktorová fyzika: laboratorní cvičení. Praha: ČVUT v Praze. 2016. ISBN 978-80-01-05904-3.

Jméno a pracoviště vedoucího práce: **Ing. Tomáš Bílý, Ph.D.**
KJR FJFI ČVUT v Praze

Jméno a pracoviště konzultanta: **Dr. Andrea Salvini**
LENA – Applied Nuclear Energy Laboratory, University of Pavia

Datum zadání diplomové práce: 14. 10. 2022
Datum odevzdání diplomové práce: 3. 5. 2023
Doba platnosti zadání je dva roky od data zadání.

V Praze dne 14. 10. 2022

prof. Ing. Tomáš Trojek, Ph.D.

Garant studijního programu

Ing. Jan Rataj, Ph.D.

Vedoucí katedry

ČESKÉ VYSOKÉ UČENÍ TECHNICKÉ V PRAZE
Fakulta jaderná a fyzikálně inženýrská
-3-

doc. Ing. Václav Čuba, Ph.D.

Děkan

Declaration

I declare that this thesis has been composed solely by myself and that it has not been submitted, in whole or in part, in any previous application for a degree. Except where stated otherwise by reference or acknowledgment, the work presented is entirely my own.

In Prague , date 16.12.22

.....

Bc. Petr Kladiva

Acknowledgement

I would like to thank my supervisor Ing. Tomáš Bílý, Ph.D. for his comments, suggestions and patience. I am also thankful to Daniele Alloni Ph.D. and Dr. Andrea Salvini for the opportunity to perform an experiment at LENA facility. Last, but not least, I am very grateful to my parents for their support during the years of my studies.

Rád bych poděkoval mému vedoucímu Ing. Tomáši Bílému, Ph.D. za jeho komentáře, nápady a trpělivost. Dále jsem také vděčný Danielemu Alloni Ph.D. a Dr. Andrea Salvinimu za příležitost uskutečnit experiment v zařízení LENA. V neposlední řadě jsem velmi vděčný mým rodičům za jejich podporu během let mého studia.

Bc. Petr Kladiva

Title:

Spatial effects in reactivity measurements in subcritical states of research reactors

Author: Bc. Petr Kladiva

Study programme: Applications of Natural Sciences
Field of study: Nuclear Engineering
Type of work: Diploma thesis

Supervisor: Ing. Tomáš Bíly, Ph.D.
Department of Nuclear Reactors, Faculty of Nuclear Sciences and Physical Engineering, Czech Technical University in Prague
Consultant: Dr. Andrea Salvini
LENA Applied Nuclear Energy Laboratory, University of Pavia

Abstract: Measurements of reactivity in subcritical states have been proven to be influenced by spatial-energy effects that have a large impact when determining the reactivity value. That is why this diploma thesis aims at the research of the methods for corrections of spatial effects in subcritical reactivity measurement. The work also presents the results and discussion of the Modified Source Method application at TRIGA Mark II reactor. This method was able to decrease the reactivity spatial discrepancies in comparison with the classic Source Method. Moreover, the thesis proposes a new method for online reactivity monitoring based on the Artifical Neural Network. This method and its workflow are described. The method proved the viability of online reactivity monitoring based on machine learning.

Key words: Reactivity, Subcritical state, Artifical Neural Network, Modified Source Method, Subcritical Reactor

Název práce:

Prostorové vlivy při měření reaktivity v podkritických stavech výzkumných reaktorů

Autor: Bc. Petr Kladiva

Abstrakt: Bylo prokázáno, že měření reaktivity v podkritických stavech je ovlivněno prostorově-energetickými jevy, které mají velký vliv při určování hodnoty reaktivity. To je důvodem, proč se tato diplomová práce zaměřuje na zkoumání metod určených pro korekci prostorových vlivů v měření podkritické reaktivity. Dále práce prezentuje výsledky a diskusi aplikace modifikované metody násobení zdroje na reaktoru TRIGA Mark II. Tato metoda byla schopna snížit prostorové nesrovnalosti v porovnání s klasickou metodou násobení zdroje. Navíc, tato práce navrhuje novou metodu k online měření reaktivity založené na umělé neuronové síti. Tato metoda a její postup práce jsou popsány. Tato metoda prokázala proveditelnost online měření reaktivity založeného na strojovém učení.

Klíčová slova: Reaktivita, Podkritický stav, Umělá neuronová síť, Modifikovaná metoda násobení zdroje, Podkritický reaktor

Contents

List of Figures

List of Tables

Introduction

The reactivity measurement is a frequent task especially at research reactors that are operated also in subcritical states. It has been proven in many works that the spatial effects play not negligible role in the determination of the reactivity in subcritical states. Most commonly, the online reactivity monitoring of the research reactors and subcritical assemblies is performed by the inverse point kinetic equation that takes into account various simplifications, among which the most important is that the reactor is considered as a point. That implicates that the change in neutron flux is constant in every position of the reactor. On the other hand, it is very important to monitor the reactivity also in the commercial nuclear reactors during refueling and in the spent fuel pool.

As shown in the previous works [1][2] on the topic of spatial effects in the subcritical reactor, the neutron flux is strongly dependent on the neutron source positions (either fuel or external neutron source) and on the neutron absorber positions. It should be denoted that it is the neutron spectrum that is different for every position of the reactor and that it can be referred to this problem as spatial-spectrum effects.

There has been a few ways proposed to deal with the spatial-spectrum effects. In general, one of the approaches is to find correction factors for each position of the measurement and than use the inverse kinetic equation. Another method to solve the spatial correction for steady-state subcritical states is by the Modified Source Method based on the computation of the detector efficiency in the Monte Carlo code. A different way to confront the problem is to compute the correction factors based on the detector neutron flux depending on the adjoint flux. A method that deals with the spatial effects in subcritical systems driven by a pulse neutron source is also described. Lastly, a newly suggested method for online reactivity monitoring based on the Artificial Neural Network is proposed. This method suggested by the author of the thesis is based on the collection of the measurement data and performing Serpent2 calculations. Afterwards the Artificial Neural Network is trained on the operational histories of the reactor. All spatial corrections of the reactivity measurement are described in the thesis from the physical point of view together with their advantages and limitations.

The aim of this work is to find, evaluate and compare methods for online reactivity measurement that could be implemented in research reactors. Two of the described methods were implemented and discussed in two research reactors. The Modified Source Method was successfully applied in TRIGA Mark II research reactor in Pavia, Italy. The results from the measurement are presented in chapter 2 of this work.

Chapter 3 presents a newly suggested method for online reactivity monitoring based on the Artifical Neural Network. The method and the workflow are described and the results together with Python codes for online reactivity measurement are presented.

Lastly, the results from the two research reactors are discussed and the investigated methods are compared.

Chapter 1

Methods of reactivity measurements and their spatial corrections

In this chapter, various methods of reactivity measurement are described and compared. Generally the reactivity of the subcritical system can be determined either by solving kinetics equations or by the various methods developed in the past, such as Rod-Drop, Source-Jerk, (Modified) Source Multiplication Method or Reactor Period Method. As Blaise mentions in [3], there are three ways, in general, to determine the reactivity and they can be divided into the categories:

- Static or quasi-static
- Dynamic
- Neutron noise methods

It is important to know that the subcritical measurements by the techniques mentioned above belong to the category of static or quasi-static as they always compare reactivities in a known and perturbed states and both are considered as stationary. This represents the first obstacle that must be tackled to design an online reactivity measurement for transient processes.

Solving the classic point kinetic equation is considered as the dynamic method to determine the reactivity. This reactivity is sometimes called dynamic reactivity and it is proportional to the static reactivity through the correction factor. This chapter describes both the dynamic and static methods and their combinations to determine the reactivity. Moreover, a method for subcritical reactivity measurement of the neutron pulse source driven systems is described.

Some of the dynamic methods, such as Dynamic Rod Worth measurements and its variations developed by various researchers, are used nowadays for Pressurized Water Reactor start-ups [4].

The noise techniques, such as Feynman-alpha or Rossi-alpha, are used in accelerator driven systems and are not subject of this work [5].

This chapter focuses especially on correction techniques of the spatial effects for various reactivity measurement methods.

1.1 Point kinetics equations solutions

The first section describes the point kinetics equations, as they are fundamental to understanding the nuclear reactor behaviour. This section also presents the list of the various methods that have been developed to solve the point kinetics equations.

The point kinetic equations can be derived either from the nonstationary one group diffusion equation [6] or from the Boltzman time-dependant adjoint transport equation coupled with the precursors balance equations [7]. The point kinetics equations, with the main constraints on one energy group of neutrons and treating the whole reactor as one point in terms of the neutron density $n(t)$ distribution, describe the time behaviour of the neutron density with dependence on the reactivity $\rho(t)$ as follows:

$$\frac{dn(t)}{dt} = \frac{\rho(t) - \beta_{ef}}{\Lambda} \cdot n(t) + \sum_{i=1}^{N_d} \lambda_i \cdot c_i(t) + S \tag{1.1}$$

$$\frac{dc_i(t)}{dt} = \frac{\beta_{ef,i}}{\Lambda} \cdot n(t) - \lambda_i \cdot c_i(t) \tag{1.2}$$

where $\beta_{ef} = \sum_{i=1}^{N_d} \beta_{ef,i}$ stands for the effective delayed neutron fraction, $\beta_{ef,i}$ stands for the effective delayed neutron fraction of the i-th group of the delayed neutron group precursors. Capital N_d is the number of groups of the delayed neutron precursors, λ_i is the decay constant of the i-th group precursors, Λ is the integral parameter of the mean neutron generation lifetime, c_i is the group concentration of the i-th group precursors and S stands for the neutron source. In general, the source term, the effective delayed neutron fraction, and the mean neutron generation lifetime can be time dependent during the transient. The number of the point kinetic equations is $N_d + 1$ but generally, it is common to use the 6 delayed neutron groups approximation.

The most used and common method for online reactivity monitoring in research reactors is the inverse kinetics methods. It can be derived straight from the equations 1.1 and 1.2 by imposing the initial condition $c_{i0} = \frac{\beta_{ef,i} n_0}{\Lambda \lambda_i}$, where n_0 is the initial neutron density. One can obtain then the inverse kinetic equation in the form of:

$$\rho(t) = \beta_{ef} + \frac{\Lambda}{n(t)} \frac{dn(t)}{dt} - \frac{\Lambda S}{n(t)} - \frac{1}{n(t)} \sum_{i=1}^{m} \lambda_i \cdot [\beta_{ef,i} e^{-\lambda_i t} \int_0^t n(u) e^{\lambda_i u} du + \frac{\beta_{ef,i} n_0}{\lambda_i} e^{-\lambda_i t}] \tag{1.3}$$

The solution of the equation above is used for the online reactivity monitoring system in the research reactors, and it is computed by a numerical algorithm. The important constants λ_i and $\beta_{ef,i}$ can be computed by Monte Carlo codes.

Other point kinetic solutions are well mentioned in the article [8] that moreover, describes the implementation of the physic-informed neural network on the solution of the point kinetic equations. This method is based on the training of the neural network that takes the physics differential equations as a regularizer in the loss function, that is used to define the optimisation problem equivalent to the solution of the original differential equations. Together with converged accelerated Taylor series [9] and with enhanced piecewise constant approximation method [10] it achieved very high accuracy in solving the point kinetics equations. The other methods are based on different mathematical background such as trigonometric Fourier-series solutions, ITS2 method, Magnus expansion, analytical exponential model to solve the stochastic point kinetics equations via eigenvalues and eigenvectors and many more are mentioned with their references in [8]. It should be noted that these methods are dealing with a differential equation numerical solution and do not mention or take into account the neutron count rates measurement, thus they cannot be used for the online reactivity measurement.

Although these methods proved as successful in solving the point kinetic equations, they do not deal with the spatial corrections and the main problem remains in the physics itself of the point kinetic equations, namely, in the constraints on one energy group of neutrons and the point behaviour of the reactor. Therefore the point kinetics model introduce the modelling error itself.

Extended Kalman filter application for reactivity measurement

One of the problems during the online reactivity measurement through the inverse kinetics equation solution is the fluctuation of the neutron signal in the detectors. This can be overcome by the so-called Extender Kalman filter (EKF), which is a widely used algorithm used for the estimation of the non-linear systems [11], which an inverse kinetics equation is. EKF is a more advanced version of the Kalman filter including the first order approximations in the Taylor expansion. [12] Generally, it is a technique working with a time measurement that include statistical noise and variance values to produce the estimation of the unknown variable [11].

The article [12] deals with an online subcritical reactivity measurement based on point kinetics equations with the external neutron source with the application of the EKF technique. Importantly, it proves that the statistical fluctuation in the count rates measurement with the inverse point kinetics in the region of the low count rates strongly affect the estimation of the reactivity. EKF technique application has shown a notable decrease in the fluctuation even when the count rates decreased almost to zero. A graph in Fig.1.1 from the study [12] of the Rod-Drop reactivity measurement proves the smoothing of the detector signal and also reactivity determination determined from the neutron count rates.

The authors mention that the reactivity estimation by the EKF technique was significantly more accurate, but on the other hand they admit that the source term in the inverse kinetic equation and the detector efficiency must be modified to capture the spatial effects during the reactivity measurement, and further study should be conducted.

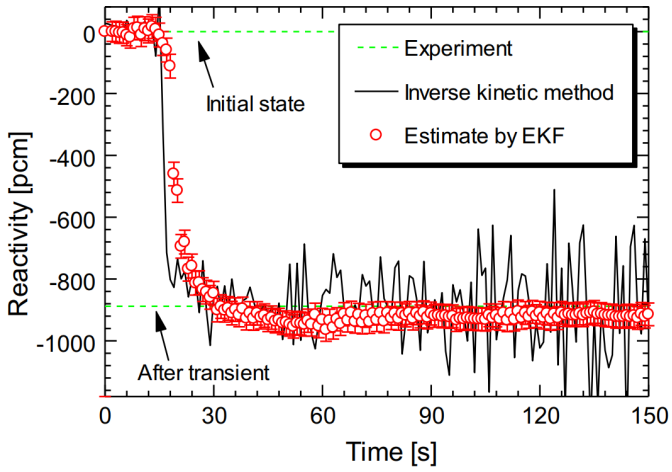

Figure 1.1: Comparison of the reactivity determination by the inverse kinetic method and EKF during the Rod-Drop experiment from [12]

Multipoint kinetics solution

The one point kinetics section is extended by a multipoint kinetics approach that has been under research but still seems not to be used for reactivity measurement. This method, as the name suggests, is an extension of the one point kinetic model. Generally, multipoint equations are based on the subdivision of the reactor phase space into separated subdomains for which the coupling terms are determined. Each subdomain then with its physical characteristics behaves as a point-like system. Individual subdomains are connected through boundary conditions in terms of the probabilities per unit time that the neutron is introduced into the subdomain or that a neutron has originated in the subdomain or that a neutron has leaked from the subdomain. It is a complex system of coupled first-order ordinary differential equations which number depend on the number of subdivisions made. Generally neutrons stream between the subdomains not only in space, but also in energy groups. [13]

A simple two-zone, one energy group model can be described as:

$$\begin{aligned} \frac{dn_1}{dt} &= \nu(a_{11}n_1 + a_{12}n_2) - c_1 n_1 \\ \frac{dn_2}{dt} &= \nu(a_{21}n_1 + a_{12}n_2) - c_2 n_2 \end{aligned} \tag{1.4}$$

where ν is the yield of the new neutrons, a_{11} is a probability per unit time that neutron has been induced in zone 1, a_{12} is a probability per unit time that neutron has originated in zone 2 but has been induced into the zone 1, c_1 describes the leakage of the neutrons from the zone 1. The notation is analogous for the zone 2.

In general, equations of the multipoint kinetic model with one energy group with delayed neutrons can be described as follows:

$$\frac{d\vec{n}}{dt} = \nu(1-\beta)\mathbb{A}\vec{n} - \mathbb{C}\vec{n} + \sum_{i=1}^{N_d} \lambda_i \mathbb{C}^{(i)}$$
$$\frac{d\mathbb{C}^{(i)}}{dt} = \beta_i \nu \mathbb{A} - \lambda_i \mathbb{C}^{(i)} \tag{1.5}$$

where matrices have the analogous meaning as the letters in the notation in equations 1.4, N_d is the number of delayed neutron groups and $\beta = \sum_{i=1}^{N_d} \beta_i$ is a fraction of the delayed neutrons. In general, all zones of the subdivision are coupled, not only the neighbours. Evaluation of the coefficients can be done using the Monte Carlo code and in the study [13] a 6 zone heterogeneous zone in MCNP has been evaluated. The characteristic mean absorption times Λ_z have been calculated for each zone together with the probabilities of the leakage, capture, fission, and zone-to-zone transmission. A multi-energy group for Multipoint kinetics theory is also presented in the study [13].

Generally, it has not been found that the multipoint kinetics model had ever been used for reactivity measurement yet for the complexity of the equations. It should be noted that in the realistic cases, the material properties during the transient processes are changing and thus the physical parameters of the subdomains should be updated. Anyway in its generality, the multipoint approach could be used for reactivity measurement and deal with the spatial effects. [13]

1.2 Modified Source Multiplication Method

The first method that deals with the spatial correction in the reactivity measurement is the Modified Source Multiplication Method that has been tested in the previous work [2] and has been proven as successful in terms of the determination of the reactivity in dependence on the position of the measurement. The main drawback is that the reactivity can be corrected only in the steady subcritical state as the method itself requires the reactivity and reaction rates to be computed by Monte Carlo code. In the previous work the method has been tested on the zero-power reactor VR-1 and this thesis aims to test the method on the reactor Triga Mark II in Pavia, Italy.

This method can be successfully used during the fuel reloading or during other operations in the subcritical reactor that deal with the steady subcritical states.

The method is based on the correction of the classical Neutron Source Multiplication Method for reactivity determination that is derived from the point kinetics assumptions. In principal this method estimates the subcritical reactivity regardless on the position of the detector by comparing the detector count rates and reaction rates change given by Monte Carlo neutron transport code. [14]

It needs a reference reactivity to be computed or measured by an arbitrary method such as, Source-Jerk, Rod-Drop or Reactor Period Method. As proven in [2], it

is important to choose the subcritical reference state and a method to determine the reference subcritical state. In the previous work, the highest correspondence in the determination of reactivity regardless of the position was with the Source-Jerk method. This obtained result depends on the experimental set-up, and therefore it is not generally the best method to be chosen. It is important to bare in mind that also the methods for determining the reactivity above are usually based on the point kinetics equations and that brings an implicit error into the calculation. Alternatively, the reference state can be computed from the high-fidelity Monte Carlo code, and the count rates on the detectors for the specific subcritical states would be measured during the experiment. [15] In that case, the determination of reactivity would no longer depend on the point kinetics model.

Generally, the method derived by Tsuji [16] describes the reactivity of the arbitrary subcritical state ρ_i with respect to the above mentioned reference subcritical reactivity ρ_{ref} as follows:

$$\rho_i = C_i^{im} C_i^{sp} C_i^{ext} \frac{N_{ref}}{N_i} \rho_{ref} \tag{1.6}$$

Where C_i^{im}, C_i^{sp}, C_i^{ext} are the corrections factors of the method and N_i, respectively N_{ref} are the count rates measured in the steady-static subcritical states. To describe the correction factors, it is important to understand the calculation methods implemented in the computational codes. Physically, the reactor is critical if in the absence of an independent neutron source a steady state neutron population is set. That cannot be accomplished in the calculations when it is dealt with the subcritical reactor, that is why in the iterated fission source method (or k-eigenvalue method) a correction factor (the eigenvalue) is artificially introduced into the neutron balance equation and so that an artificial steady state can be obtained. The neutron balance equation is then solved as an eigenvalue problem, and it is common to introduce the eigenvalue to the fission term. The eigenvalue is then defined as $\lambda = \frac{1}{k}$ and it is the highest value of k and its corresponding eigenmode that makes the system critical. [7][15] This can help to understand the term C_i^{ext} in the equation 1.6 because this factor is important to extract the fundamental mode component that depends on the state of the reactor and can generally change between the reference and measured subcritical state. The other factor C_i^{im} imposes the difference of importance between source neutrons in the reference and measured state and is given by the adjoint flux function (also called importance function). It helps to take into account the fact that in the deep subcritical states the source neutrons are relatively more important than in the nearly critical states. Finally, the most important factor C_i^{sp} takes into account the change of the neutron flux distribution in the different subcritical states given by, the most commonly, the change of absorbers in the core. [15] The theoretical study of the factors mentioned above depending on the reactivity and neutron source distribution is in [15]. Among other conclusions, it is stated that with an asymmetric point neutron source, the subcriticality estimated without the correction factors heavily depends on the position of the neutron detector. Lastly, it should be mentioned that the equation 1.6 without the correction factors would be the classic neutron source multiplication equation based on point kinetics to

estimate reactivity.

The complete derivation of the modified source multiplication method is in [15] or [16]. It is derived from the multigroup diffusion equation and its adjoint form together with multigroup diffusion equation with the source term. The solution is found due to the assumption that the eigenfunctions form a complete and orthogonal basis and only one fundamental mode exists in the reactor. The detector is characterized by its cross-section Σ_d at the position $\vec{r}_d$. The most general formulation of the reactivity given by the modified source multiplication method can be found as:

$$\frac{\rho^s_{m,i}}{\rho^s_{m,ref}} = \left[\frac{(\phi^*_{c,i}, S_i)}{(\phi^*_{c,ref}, S_{ref})}\right] \left[\frac{\frac{\Sigma_d \phi_{c,i}}{(\phi^*_{c,i}, \mathbb{F}\phi_{c,i})}}{\frac{\Sigma_d \phi_{c,ref}}{(\phi^*_{c,ref}, \mathbb{F}\phi_{c,ref})}}\right] \left[\frac{\frac{(\phi^*_{c,ref}, \mathbb{F}\phi^s_{c,ref})}{(\phi^*_{c,ref}, \mathbb{F}\phi_{c,ref})} \frac{\Sigma_d \phi_{c,ref}}{N_{ref}}}{\frac{(\phi^*_{c,i}, \mathbb{F}\phi^s_{c,i})}{(\phi^*_{c,i}, \mathbb{F}\phi_{c,i})} \frac{\Sigma_d \phi_{c,i}}{N_i}}\right] \frac{N_{m,ref}}{N_{m,i}} \tag{1.7}$$

The brackets successively refer to the correction factors C^{im}_i, C^{sp}_i and C^{ext}_i respectively. In the equation 1.7, the notation is following: the lower index m denotes the measured quantity in the reference (ref) or i-th subcritical state. N with its indexes stands for the count rate measured at the detectors. The lower index c denotes the quantities that are computed by a proper computational tool such could be a Monte Carlo code. The neutron flux is denoted as ϕ and the adjoint flux is labelled as ϕ^*. $\mathbb{F}$ is the production (fission) operator and S with its index is the neutron source distribution during its subcritical state.

Due to the computational burden the correction factor from 1.7 is usually simplified to the form of [3]:

$$\frac{\rho_{m,i}(\vec{r}_d)}{\rho_{m,ref(\vec{r}_d)}} = f_{MSM}(\vec{r}_d) \frac{N_{m,ref}(\vec{r}_d)}{N_{m,i}(\vec{r}_d)} = \frac{\rho_{c,i}}{\rho_{c,ref}} \frac{N_{c,i}(\vec{r}_d)}{N_{c,ref}(\vec{r}_d)} \frac{N_{m,ref}(\vec{r}_d)}{N_{m,i}(\vec{r}_d)} \tag{1.8}$$

where the correction factor f_{MSM} takes into account the change in the detector efficiency and source distribution between two subcritical states. In this equation, $N_{c,i}$ stands for the calculated reaction rates in the detector position. The vector $\vec{r}_d$ is present in the equation to emphasize the importance of the position of the measurement. Satisfactory results were achieved with the equation 1.8 for example in [3] [14] [17] [2]. On the other hand, it should be mentioned that in [4] is the correction factor simplified to the form as in 1.9, and higher correspondence among the places of measurement is achieved in case when the adjoint flux is considered and computed.

$$\frac{\rho_{m,i}(\vec{r}_d)}{\rho_{m,ref(\vec{r}_d)}} = \frac{(\phi^*_{c,i}, S_i)}{(\phi^*_{c,ref}, S_{ref})} \frac{\Sigma_{d,i}\phi_{c,i}(\vec{r}_d)}{\Sigma_{d,ref}\phi_{c,ref}(\vec{r}_d)} \frac{(\phi^*_{c,ref}, \mathbb{F}\phi_{c,ref})}{(\phi^*_{c,i}, \mathbb{F}\phi_{c,i})} \frac{N_{m,ref}(\vec{r}_d)}{N_{m,i}(\vec{r}_d)} \tag{1.9}$$

It is interesting to mention that the adjoint flux cannot be in the Monte Carlo codes computed directly and with the problem is dealt in a following way: It has been proven in [18] that the adjoint flux is proportional to the so-called Iterated Fission Probability and as the adjoint flux is in 1.9 in the fraction, the Iterated Fission

Probability $I_{FP}(\Theta)$ can be computed for each subcritical state and the ratio of the them can be used as the ratio of the adjoint fluxes. It is sometimes referred to the adjoint flux as to the importance function of the neutrons in the given position. Therefore, the Iterated Fission Probability $I_{FP}(\Theta)$ in the corresponding position of the phase-space $\Theta = (\vec{r}, E, \vec{\Sigma})$ is computed by introducing a single source neutron in $\Theta = (\vec{r}, E, \vec{\Sigma})$ and an asymptotic population size resulting from the introduction of the single neutron is followed [19]. Practically, it is then computed as the product of the multiplication coefficients (see 1.10) for λ generations of the neutrons until the $\phi^{(\lambda)}$ converges to its fundamental mode.

$$I_{FP}^{\lambda}(\Theta) = k_{eff}^{(1)} k_{eff}^{(2)} ... k_{eff}^{(\lambda-1)} k_{eff}^{(\lambda)} \tag{1.10}$$

As it was mentioned in the introduction of the chapter, Modified Source Multiplication Method belongs among the static or quasi-static reactivity determination techniques. Although a correction factor $f_{MSM} = f_{MSM}(\rho)$ can be found as a function of reactivity, as for instance in [14]. Modified Source Method cannot be used for the online reactivity measurement correction because a quasi-static state would be needed to measure the count rates. Modified Source Method is designed for determination of the static or quasi-static subcritical measurements and cannot be applied for reactivity determination in transient processes.

1.3 Reactivity measurement based on the shape function of the detector neutron flux depending on the adjoint flux

This section aims to describe the technique proposed in [4] to compute in advance the correction factors for the reactivity measurement through the inverse kinetic equation 1.3. The mentioned study proposes to compute the correction factors for the so-called Dynamic Rod Worth Measurement technique, that importantly deals with the transient process of the large reactivity insertion of over 2000 pcm. The author of this thesis suggests developing the technique that is described in this section on the whole online reactivity measurement.

The main idea of the method is to compute the correction factors for the transient process, depending on the shape function of the detector neutron flux, without calculating the neutron detector response function. Correction factor is applied directly to the neutron detector flux amplitude function, that is an input for the inverse kinetic equation. This method aims to correct the spatial effects given by the changes in the neutron flux shape and neutron spectra during the transient processes occurring in the subcritical reactor. During the fast transient processes, the perturbation may be affected by rapid changes in the neutron flux and that is why it can affect the accuracy of the correction factors.

The output of the method in the study [4] is a dependence of the correction factor on the position of the rod during the Dynamic Rod Worth Measurement. This thesis

aims to suggest a method that could compute the correction factor dependence on the position of the all the control rods needed to reach the critical state. The main drawback of this technique is demanding computational time, especially to calculate the so-called Iterated Fission Probability, proportional to the adjoint flux as mentioned in the text before.

The method results in an improvement of the measured reactivity depending on the spatial effects but on the other hand, it is still influenced by the point kinetics physics model and its constants.

Methodology

The methodology described in this section is adopted from the study [4]. The main idea to correct the input into the online reactivity monitoring is based on computing the correction factors of the amplitude function $p(t)$. In the point kinetics equation 1.3, the neutron density $n(t)$ is considered, but as it is impossible to measure the neutron density during the operation of the reactor, $n(t)$ is considered as the neutron detector signal (count rates of neutrons coming to the volume of the detector and reacting in it). That is why the neutron density or neutron detector signal can and is in the equation 1.3 replaced by the amplitude function $p(t)$.

One point kinetics assumptions allow to describe the time dependent neutron flux $\phi(\vec{r}, E, t)$ as the product of the amplitude function $p(t)$ and the shape function $\psi(\vec{r}, E)$:

$$\phi(\vec{r}, E, t) = p(t)\psi(\vec{r}, E) \tag{1.11}$$

where the shape function is considered unchanged during the measurement. Time t is considered as time during the transient process, therefore, practically the state of the reactor at given time t_0 can be considered as subcritical or critical state of the reactor given by the absorbers (mainly rods) position in the core. Therefore, later in this section the time dependence of the neutron flux $\phi(\vec{r}, E, t)$ will be discretized according to the position of the rods in the reactor.

From the equation 1.11 it can be seen that also the detector neutron flux $\phi(\vec{r}_d, E, t)$ is proportional to the amplitude function $p(t)$. As shown in previous studies (e.g.: [1]) and during operational experience, the shape function of the flux is time-dependent during the transient processes and that is why the detector neutron flux $\phi(\vec{r}, E, t)$ is affected by the changes in the shape of the neutron flux $\psi(\vec{r}, E, t)$. That is in contradiction with the equation 1.11 and for that reason, the correction factor aims to correct the neutron signal.

It should be mentioned that the study in [4] proposes the correction (i) of the neutron flux amplitude function, (ii) the static-dynamic correction given as in 1.12. The static-dynamic correction describes the relation between the dynamic reactivity that is determined by the inverse kinetics equation with the spatial corrections as described bellow and the static reactivity that can be computed from the classic k-eigenvalue problem for instance in Monte Carlo transport codes. The researchers

in [4] searched for correction factors as in equation 1.12 by comparing the static results of MCNP and the dynamic results given by simulating a transient analysis of the proposed Rod-Drop experiment. This thesis does not aim to find the dynamic correction factors C_{dyn}.

$$\rho_{st} = C_{dyn}\rho_{dyn} \tag{1.12}$$

Detector signal correction

To capture the changes in the flux shape functions during the transient processes, the detector signal correction is proposed. According to the exact point kinetics discussed above, the neutron flux shape in the reactor $\phi(\vec{r}, E, t)$ can be written as:

$$\phi(\vec{r}, E, t) = p(t)\psi(\vec{r}, E, t) \tag{1.13}$$

Note that the neutron flux shape function $\psi(\vec{r}, E, t)$ is the function of time, in other words it is a function of the rods position during the transient process and also the rods movement velocity (the delayed neutrons presence, that influence the flux shape, in the reactor is not given only by the rods positions but also by the velocity of the change of the position).

The neutron signal in the detector position $n_{det}(t)$ according to the theory of the nuclear reactors [20] can be written as:

$$n_{det}(t) = \int_V \int_E w(\vec{r}, E)\phi(\vec{r}, E, t)dEdV \tag{1.14}$$

where V is the volume of the whole reactor, E is the energy spectrum of neutrons in the reactor and $w(\vec{r}, E)$ is the spatial weighting function of the detector. The method described here is innovative because it avoids computing the spatial weighting function of the detector. That itself is a very complex problem and several studies have been developed on this topic and can be found in [21] [18] [22]. The weighting function $w(\vec{r}, E)$ denotes the neutron contribution at the position $\vec{r}$ in the reactor. There is a degree of freedom in defining the weighting function and for instance in [22] it is a value that represents the average number of reactions that occurred in the detector per one source neutron created in a specific volume of a fuel pin. It should also be mentioned that the accuracy when computing the weight function is given by the fineness of the mesh.

One can rewrite the equation 1.14 and obtain:

$$n_{det}(t) = \int_V \int_E w(\vec{r}, E)p(t)\psi(\vec{r}, E, t)dEdV \tag{1.15}$$

So, the neutron flux amplitude function $p(t)$ can be factorized and is given as:

$$p(t) = \frac{n_{det}(t)}{\int_V \int_E w(\vec{r}, E)\psi(\vec{r}, E, t)dEdV} \tag{1.16}$$

The neutron signal $n_{det}(t)$ is also given by the neutron flux in the detector $\psi(\vec{r}_d, t)$ and the detector sensitivity $\Sigma(t)$ as:

$$n_{det}(t) = \Sigma(t)\phi(\vec{r}_d, t) = \Sigma(t)p(t)\psi(\vec{r}_d, t) \tag{1.17}$$

where $\psi(\vec{r}_d, t)$ is the shape part in the detector position. To avoid computing the weight function $w(\vec{r}, E)$, the equations 1.17 and 1.15 are used and the amplitude function can then be expressed as:

$$p(t) = \frac{n_{det}(t)}{\Sigma(t)\psi(\vec{r}_d, t)} \tag{1.18}$$

Instead of using the weight function $w(\vec{r}, E)$, it is the shape part of the detector neutron flux $\psi(\vec{r}_d, t)$ used to correct the amplitude function $p(t)$.

Generally, the shape function can be described as in 1.19, which is also in correspondence with 1.11. The same can be applied only on the detector position $\vec{r}_d$.

$$\psi(\vec{r}, E, t) = \frac{\phi(\vec{r}, E, t)}{C(t)} \tag{1.19}$$

The correction of the neutron signal is given with respect to the critical state values denoted by the lower index cr and is proposed as:

$$\overline{p}(t) = \frac{p(t)}{p_{cr}} = \frac{n_{det}(t)}{n_{cr}}\frac{\Sigma_{cr}}{\Sigma(t)}\frac{1}{C_{det}} = \frac{n_{det}(t)}{n_{cr}}\frac{1}{C_{det}} \tag{1.20}$$

where the assumption that the detector sensitivity during $\Sigma(t)$ does not change during the transients is taken into account. It is given by the assumption that the neutron energy spectra stay unchanged at the detector position during all the subcritical and critical states. This assumption can lead to differences in measured reactivity and the real value. The corrected neutron amplitude $\overline{p}(t)$ is taken as an input into the online reactivity monitoring.

The correction factor of the detector signal is given as:

$$C_{det} = \frac{\psi(\vec{r}_d, t)}{\psi_{cr}(\vec{r}_d)} \tag{1.21}$$

Neutron flux shape function $\phi(\vec{r}, t)$ is difficult to be obtained directly from a transport calculation and it is proven in [4] that the adjoint flux of the critical state $\phi^*_{cr}(\vec{r}, E)$ fulfils the requirements for the weighting function of the neutron flux

$\phi(\vec{r}, E, t)$ to compute the neutron flux shape. It can be explained in two ways why the adjoint flux is chosen. Firstly, in static perturbation theory, the adjoint flux function is used to eliminate the first order reactivity perturbation. Secondly, the adjoint flux function is sometimes called an importance function and its meaning can be described as the importance of a neutron in a given position at given time with a given energy. To compute the adjoint flux directly, the transport equation would have to be computed backwards in time. In other words, the adjoint flux helps to retrieve the information at the end of the process and in the considered situation, the end process is the critical state. It should be reminded that the method aims to observe and correct the changes in the neutron flux shape between the subcritical and critical states.

Finally, the part of the shape function is given by the following equation:

$$\psi(\vec{r}_d, t) = \frac{\phi(\vec{r}_d, t)}{\int_V \int_E \frac{\phi_{cr}(\vec{r},E)^* \phi(r,E,t)}{v(E)} dEdV} \tag{1.22}$$

where $v(E)$ is the velocity of the neutron. Note that the integral is over the space of the whole reactor and over the neutron energy spectrum. Finally, the correction of the neutron amplitude is given by equations 1.22 and 1.20:

$$\overline{p}(t) = \frac{n_{det}(t)}{n_{cr}} \frac{\psi_{cr}(\vec{r}_d)}{\phi(\vec{r}_d, t)} \int_V \int_E \frac{\phi^*_{cr}(\vec{r}, E)\phi(\vec{r}, E, t)}{v(E)} dEdV \tag{1.23}$$

where $\psi_{cr}(\vec{r}_d)$ is:

$$\psi_{cr}(\vec{r}_d) = \frac{\phi_{cr}(\vec{r}_d)}{\int_V \int_E \frac{\phi^*_{cr}(\vec{r},E)\phi_{cr}(\vec{r},E)}{v(E)} dEdV} \tag{1.24}$$

The correction of the amplitude 1.23 is applied to the online reactivity monitoring in the inverse kinetic equation 1.3 where $\overline{p}(t)$ is considered instead of the input parameter $n(t)$.

Suggested online reactivity monitoring application

The author of the thesis develops on the method described above and suggests how to compute the correction factor, then how the integrals in the equation 1.23 should be discretized and how each value in the equation 1.23 could be obtained.

The number of energy groups g must be chosen, and the mesh must be discretized to compute the average neutron fluxes in each mesh element. The quantities of the equation 1.23 will be measured/computed as:

- $n_{det}(t)$ is the value of the count rates during the transient for each detector
- n_{cr} is the average value of the count rates for the critical state

- $\phi_{cr}(\vec{r}_d)$ is the average value of the neutron flux computed by the Monte Carlo code in the volume of the detector in the critical state
- $\phi(\vec{r}_d, t)$ is the average value of the neutron flux computed by Monte Carlo code in external source mode in the volume of the detector for each transient state
- $\phi(\vec{r}, E, t)$ is the average neutron flux in the element of the mesh of a group g that can be computed by Monte Carlo code
- $v(E)$ is the neutron speed in the energy group g that can be calculated from Monte Carlo code as in equations 1.25 where the mesh and energy discretization is performed. $E_{i,up}$ and $E_{i,down}$ is the upper, respectively lower boundary of the discretized energy bin, $\phi_{i,j}$ is discretized neutron flux in l discretized volume bins and g energy groups. The velocity is then computed from the kinetic energy of the neutron with the neutron mass m. In general, the velocity of neutron in each volume element is dependent on the different neutron flux for different subcritical states (denoted by t that implicates a transient process).
- $\phi^*_{cr}(\vec{r}, E)$ is the adjoint flux of the critical state that cannot be directly computed by Monte Carlo code. The adjoint flux also needs to be discretized into g energy groups and l volume elements. The problem of the adjoint flux has been discussed in the previous parts of the work and due to its proportionality to the Iterated Fission Probability $I_{FP}(\Theta)$ the discretized value $\phi^*_{cr,i,j}$ can be computed by k-eigenvalue calculations (see equation 1.10) in Monte Carlo codes when inserting initial neutrons into the given element of the mesh with the average neutron energy of one group according to the energy discretization. The discretization must be well chosen especially because of the computational demands on a high number of the k-eigenvalue calculations.

$$\overline{E}(t) = \frac{\sum_{j=1}^{l}\sum_{i=1}^{g}\frac{E_{i,up}+E_{i,down}}{2}\phi_{i,j}}{\sum_{j=1}^{l}\sum_{i=1}^{g}\phi_{i,j}} \qquad v(t) = \sqrt{\frac{2\overline{E}(t)}{m}} \tag{1.25}$$

Finally, the author of the thesis suggests discretizing the time domain (transient process) in T subcritical states where a specific subcritical state $\tau \in \{1, 2, 3, ..., T\}$ is given by the position of the rods that are also the input for the calculations in Monte Carlo code for values listed above. The discretized value of the neutron amplitude for a given discretized transient time τ given by the rods position will be computed according to:

$$P_\tau = \frac{n_{det}(t)}{n_{cr}}\frac{1}{C_{det,\tau}} = \frac{n_{det}(t)}{n_{cr}}\frac{\psi(r_d)}{\phi_\tau(r_d)}\sum_{j=1}^{l}\sum_{i=1}^{g}\frac{I_{FP}(i,j)\phi_{i,j,\tau}}{v_i} = n_{det}(t)\tilde{C}_{det,\tau} \tag{1.26}$$

where part of the shape function in the volume of the detector $\psi(r_d)$ is discretized as:

$$\psi(r_d) = \frac{\phi_{cr}(r_d)}{\sum_{j=1}^{l}\sum_{i=1}^{g}\frac{I_{FP}(i,j)\phi_{cr,i,j}}{v_i}} \tag{1.27}$$

Note that in the equations above, it is considered that the neutron energy spectra are not changing during the transient processes which enables to compute neutron energy v_i in an energy group i not depending on the neutron flux change during different subcritical states.

The main idea in the application of this method in the research reactor is to compute the discretized correction factors $\tilde{C}_{det,\tau}$ as in equation 1.26 for various subcritical states depending on the rod positions and then fit the relation between rods positions (different subcritical states) and correction factors into a high polynomial (a high polynomial is chosen instead of the interpolation between the correction factors, in general the approach would be equivalent). A discretized value of the neutron amplitude P_τ would substitute $n(t)$ in inverse kinetic equation 1.3. The count rates $n_{det}(t)$ would be measured and the value of the current correction factor $\tilde{C}_{det,\tau}$ would be coupled with the position of the rods through the polynomial. In practise, the software of the reactimeter would be coupled with the rod positions and that is how a correction factor value could be implemented in online reactivity monitoring. The correction factor must be computed for each detector position.

1.4 Sjöstrand Area Method

Among other widely used methods, one can find the so-called Sjöstrand Area Method or sometimes just Area Method. This method for reactivity measurement is used in subcritical systems with a pulse neutron source. It has been under research for the purposes of the application in accelerator-driven systems that can be used for instance for the nuclear waste incineration.

This method requires the detector used with a fast resolution because after a neutron pulse shot a pulsed neutron source histogram is obtained for each detector. The histogram is measured in a few microseconds and the reactivity is determined from the definition of the effective delayed neutrons fraction. A short time after the pulse, only the prompt neutrons are detected in the position of the detector and after a few microseconds also the first contribution from the delayed neutrons occurs until the count rate in the detector establishes to a constant value. Then the ratio of the areas under the pulse described first by the prompt neutrons A_p and then by the delayed neutrons A_d determines the reactivity measured in β_{eff} as in equation: 1.28. [23] An example of the measurement of the pulsed neutron source histograms from [23] for three different detector positions (EC2B, EC6T, MC2) is displayed in Fig.:1.2.

$$\rho_\$ = \frac{\rho}{\beta_{eff}} = -\frac{A_p}{A_d} \tag{1.28}$$

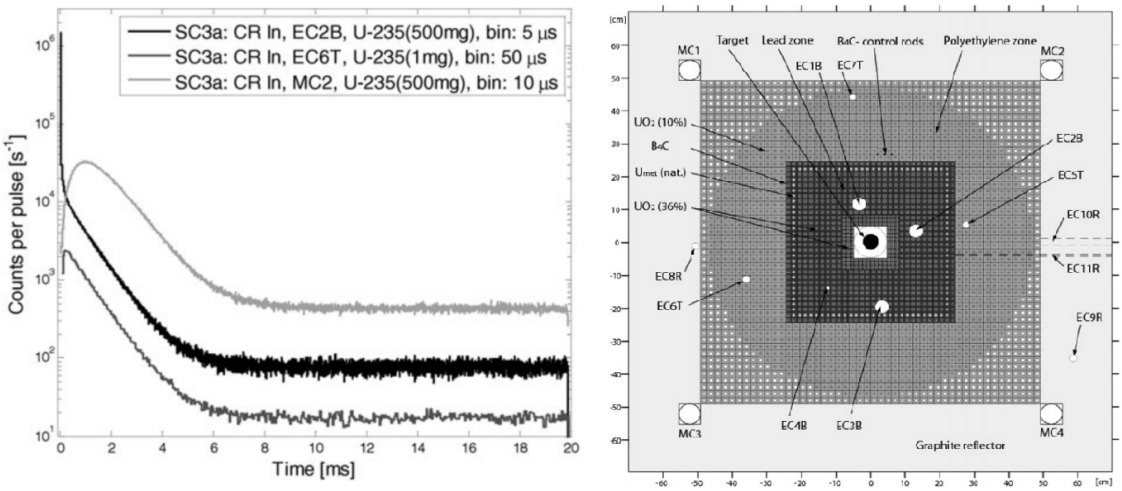

Figure 1.2: An example of the measurement of the pulsed neutron source histograms (on the left) for three different detectors positions (EC2B, EC6T, MC2) as shown in the picture on the right [23]

An important assumption to take into account is the point kinetics of the Sjöstrand Area method. It supposes that all the prompt neutrons reach the detector volume as well as the delayed neutrons. One can also observe the differences of the pulsed neutron source histograms for different detector positions in the Fig.:1.2. That is why in [23], the authors also suggest spatial corrections computed by the Monte Carlo code, MCNP in their case.

The idea of spatial correction is that one can compute a ratio of the prompt neutrons and delayed neutrons at every detector position i just by enabling or disabling the delayed neutrons in the Monte Carlo calculation. The correction factor is then given as in the equation 1.29, where $\rho_{MC,i}$ is computed as the ratio of the prompt and delayed neutrons contributions in the Monte Carlo code in the location i and ρ_{MC} is a reactivity computed from the classical k-eigenvalue calculation in the Monte Carlo code. [23]

$$C_i = \frac{\rho_{MC,i}}{\rho_{MC}} \tag{1.29}$$

The experimentally measured reactivity at the detector position i is then given as follows:

$$\rho_{exp} = \frac{\rho_{exp,i}}{C_i} \tag{1.30}$$

In conclusion, the spatial corrections in [23] led to a reduction of the data dispersion among different detectors positions. It should be once again noted that this method is applicable in the subcritical systems with a neutron pulse source.

1.5 Artificial Neural Network

This section describes an innovative technique to asses the reactivity determination problem. Artificial Neural Network (ANN) is a biologically inspired computational system that in its generality can be able to predict output of any quantity based on the training by the input data. ANNs are universal approximators of multivariate non-linear functions. The ANN method has been successfully used in a vast amount of not only scientific fields. Many types of ANN developed based on complexity. The main idea behind the ANN is that each element of an input vector $\vec{p}$ is connected to each neuron through the weight matrix $\mathbb{W}$. Then each neuron has its bias (offset) b_i, its transfer function f and an output a_i. The ANN is trained and tested on the input data $\vec{p}$ and the output data $\vec{a}$, such that the energy function (e.g. mean square error) is minimised. During testing, the weights in the weight matrix $\mathbb{W}$ are adjusted to minimize the energy function. In general, ANN can express very complicated, non-linear relations between inputs and outputs of any kind of data. [24] A simplified scheme of an ANN with R inputs and S neurons is presented in Fig.: 1.3. The input data are gathered in the so-called input layer and the output data are gather in the so-called output layer. Based on the complexity, a hidden layer can be added in between the input and output layers in order to improve the model performance. In general, multilayer networks are more powerful than single-layer networks [24].

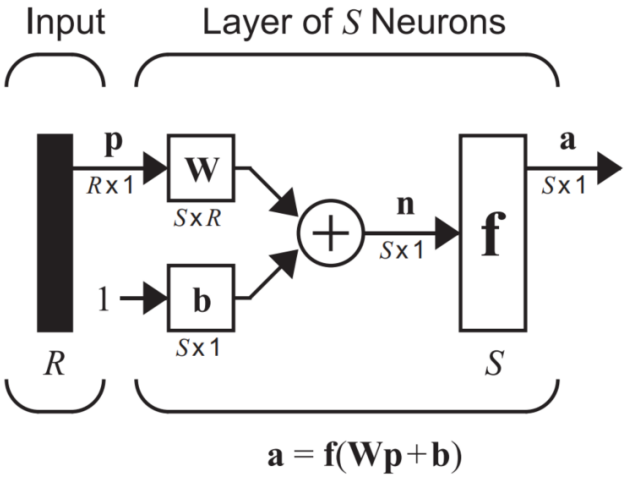

Figure 1.3: A simplified scheme of a feed-forward ANN with R inputs, 1 layer, S neurons [24]

Artificial Neural Networks has been proven as a very powerful tool with a high potential in many fields of studies thanks to their capacity to solve complex non-linear problems. ANNs enable to compute physical problems without computing a single physical equation due to the previous training and testing based on previous calculations. Thus, it can reduce also the computational demands once the ANN is well trained and tested.

In recent years, several applications of ANNs have occurred in the nuclear engineering field. For instance, in [25] the authors constructed an ANN for the dynamic processes of interactions between the reactor core and secondary coolant systems

in a pressurized water reactor (PWR) nuclear power plant (NPP). They simulated various transients with perturbation in reactivity, reactor core inlet temperature, or steam inlet temperature. Other use of an ANN in NPP with PWR is a topic of work in [26], where authors managed to built an ANN that helps to predict boron concentration and peak power factor during the core reloading. Another application of ANN in core reloading, this time in a research reactor, is evaluated in [27]. Another application of the ANN in PWR has been performed in [28] for reactivity estimation according to the total rod worth, model of Doppler effect, boron acid concentration and model of a moderator effect. Last but not least, researchers in [29] describe ANN training on the point kinetics model to predict reactivity.

Suggested ANN model for online reactivity monitoring

As the reactivity spatial corrections face many problems and seem not to be still fully resolved problem and furthermore the Artificial Neural Networks have proven to be successfully used in various scientific fields, the author of the thesis suggests building an ANN to predict reactivity during the online monitoring.

It is important to capture the physics of the processes occurring in the reactor. That is why the ANN would be informed on the basis of the physical measurement from the ex-core neutron detectors, specifically neutron count rates.

In a zero-power reactor, the reactivity is given by the position of the absorbers and fuel in the core. As discussed in the previous sections, the reactivity measurement faces many problems given by the distribution of the neutron flux, on the contrary it is considered that Monte Carlo codes should be able to predict the reactivity of the system with a very high precision. Reactivity is an integral parameter of the reactor and in Monte Carlo codes in the iterated fission source method the multiplication factor k_{eff} in the subcritical states with a source is computed by balancing the fission term by the eigenvalue $\lambda = \frac{1}{k}$. After a certain number of iterations, the calculation converges to the highest value of k that makes the system critical and it is considered as k_{eff} [7]. The Serpent2 code that is used in this thesis for the calculations has been validated for the k-eigenvalue calculations with MCNP5 in [19]. The validations in [19] are mainly with critical or near critical systems, on the other hand, a validation between Serpent2 and MCNP5 has been performed in the previous work [2] for several subcritical states of a simplified heterogeneous multiplying system. Moreover, MCNP5 calculation of the subcritical system has been also validated in the official MNCP document [30] with another calculation and very high concurrence has been reached. On the other hand the calculation of the reaction rates can be also performed in Serpent2, but calculating the reaction rates has not performed such a high concurrence as the k-eigenvalue calculations. It was shown in the previous works [1][2] or in [31] where some of the computed reaction rates reached errors up to 20 % between measurement and calculation, or in [32] where the neutron spectra and neutron flux of AmBe were compared with other computational code Nedis-2m and some relevant differences were also observed in the calculations.

That is why the ANN constructed for the prediction of the subcritical states will

be physically informed from the measurement of the detectors but the reactivity that is given by the rods position in the zero-power reactor, would be computed for various quasi-static subcritical states in Serpent2 without any constraints on the physical model such a point kinetic model. As measured count rates in the ex-core detectors fluctuate, several histories of the operation of the reactor will have to be considered for training and testing phase. Then the reactivity for the training and testing phase will be coupled with the ex-core detectors measured counting rates. Several subcritical state reactivities (given by the positions of the rods) will have to be computed. To obtain reactivity in the transient states for every rod position, the author suggests performing a polynomial fit of the control rod positions for the reactivity value for each operational history. In that case, one would be able to obtain several histories where measured count rates (physical nature of the system) would be coupled with the reactivity calculated from the Serpent2 code. It must be stressed that even though Monte Carlo codes are high fidelity codes due to the representation of real physics behaviour, the reactor models in the Monte Carlo code are created by a user under some assumptions and decisions and the reality can never be represented precisely. In other words, the suggested ANN technique relies on the absolute precision of the reactor computational model and nuclear data.

The suggested method for reactivity monitoring is a topic of chapter 3, where the method is described in more detail and the results are presented.

Chapter 2

Application of the Modified Source Multiplication Method at TRIGA Mark II reactor in Pavia

This chapter deals with the application of the Modified Source Multiplication (MSM) Method at the nuclear reactor TRIGA Mark II in Pavia, Italy. The previous chapter described several reactivity measurement methods that deal with the spatial effects during the determination. To deal with the spatial effects in TRIGA Mark II Pavia, the MSM method was chosen. The reasons why the mentioned method was chosen among others are discussed in the following text.

A multipoint kinetics solution is limited by the complexity of the equations and demands for the boundary conditions between the zones of the discretized reactor. This very complex problem could be the subject of other research work. Moreover, to verify the simulation results, a lot of precise neutron detectors would need to be inserted in various positions of the reactor core.

The reactivity measurement method based on the shape of the detector neutron flux could not have been used in TRIGA Mark II Pavia for several reasons. Firstly, it is the lack of the fast electronics that would be needed to measure the neutron count rates in the real time. Moreover, a very precise model in Serpent2 would be needed for this method. The limitations of the Serpent2 model of the TRIGA Mark II Pavia is also discussed in this chapter.

The idea to use the Artificial Neural Network on the old operational data was also mentioned in the first chapter and the method was applied at VR-1 reactor and it is described in chapter 3.

Sjöstrand Area Method could not be used for TRIGA Mark II reactor as this method is used in the accelerator driven systems.

On the other hand, MSM could have been used in TRIGA Mark II reactor in Pavia despite of lack of the online measurement reactivity instrumentation. As previously mentioned, MSM belongs to the static or quasi-static reactivity measurement method. Furthermore, a reactivity measurement of the reference state is needed.

That can be performed in TRIGA Mark II Pavia using the Rod-Drop method. As proven during the experiment, Source-Jerk cannot be performed in TRIGA Mark II Pavia because of the instrumentation settings. The neutron source is always inserted into the core and the detectors measure the source level. In case of the source extraction, the detectors stop measuring the source level and the reactor is scramed. In general, MSM could be performed in all subcritical systems where only one neutron detector is needed, then if one wants to compare the measurement results in more positions of the reactor core, at least two neutron detectors are needed.

TRIGA Mark II Pavia nuclear reactor

TRIGA (Training Research Isotope production General Atomic) Mark II nuclear reactor in Pavia in north Italy is a research reactor that reached its first criticality in 1965 at the power of 250 kW. This reactor is operated by the University of Pavia. Main purposes of the reactor nowadays are education and training, neutron activation analysis or radioisotopes production for medical and industrial applications.

The reactor is operated for more than 56 years because of high inherent safety features such as the large, prompt negative temperature reactivity feedback due to the fuel/moderator composition. The fuel rods contain the compound UZrH with the uranium enriched up to 20 % and hydrogen as the moderator. The reactor is designed as a large pool with a water column almost 5 meters above the core. Heat released during the fission reaction is removed by the natural convection, but there is also a diffuser just above the top of the core for mixing the flow, if needed, connected to the secondary and then third cooling loop. The core of diameter 44.6 cm and height 64.8 cm is surrounded by an annular graphite reflector. The core contains three control rods with different control rod weights (shim, regulating and transient). There is a RaBe neutron source in the channel F-4 [33]. See the core configuration in Fig.: 2.1.

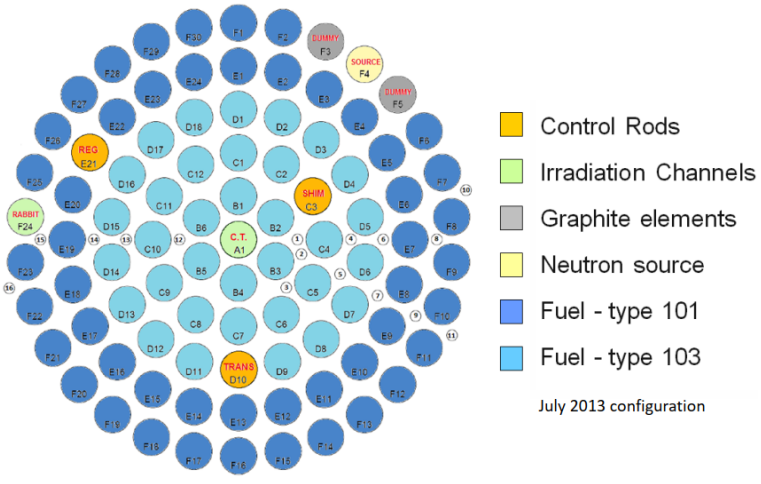

Figure 2.1: TRIGA Mark II Pavia scheme [33]

As one could observe in Fig.: 2.1, there are two types of the fuel elements in the reactor core. The fuel element type 101 contains slightly less of the UZrH compound

as the active length (35.6 cm) is a bit shorter then in type 103 (38.1 cm). The cladding of type 101 is made of aluminium, on the other hand the cladding of type 103 is made of the stainless steel. What regards the burnable poison, the fuel 101 contains two disks of burnable poison from SmO_3 in the upper and lower parts of the fuel element. In contrast to fuel 101, fuel 103 does not contain any burnable poison. Furthermore, the ratio of Zr-H in the compound of UZrH is different in the fuel types: type 101 (1:1 ratio), type 103 (1:1.6 ratio). Lastly, type 103 contains central zirconium rod, while there is none in type 101 [33].

There are three control rods in TRIGA Mark II Pavia nuclear reactor. The Shim from B_4C is the rod with the highest reactivity worth (about 3 - 3.5 β_{eff}) and the rod is motor driven. The Transient rod's worth is about 2 - 2.5 β_{eff} and its material is borated graphite. This control rod is pneumatic, and that is why during the operation the control rod can be only in the upper or bottom end position. The third control rod is Regulating designed for tuning the reactivity during the operation. Similarly to Shim, it is also motor driven from B_4C but on the other hand the reactivity worth is between 1 and 1.5 β_{eff} [33].

Experimental setup

One of the detectors used for the MSM experiment was the fission counter WL-23830 connected to the logarithmic channel of the Quad Scaler and Preset Counter Timer from CAEN. The fission chamber from Westinghouse contains very high enriched uranium as the neutron sensitive material at the sensitive length of 20.2 cm. The filling gas of the detector is mainly argon and the case and electrode materials are aluminium [34].

The other detector is an uncompensated triaxial ionization chamber WL-23934 also from Westinghouse. The ionization chamber sensitive material is ^{10}B at the active length of 8.6 cm. The gas filled in the detector is hydrogen and the chamber electrodes are also made of aluminium [35]. The ionization chamber is connected to the power level measurement. During the operation of the reactor, the voltage from the chamber is recorded in the range of 0 to 10 mV depending on the range of the logarithmic power switch. Then if needed, the power can be computed from the voltage value.

The detectors are during the operation outside of the reflector, the scheme is in Fig.: 2.2.

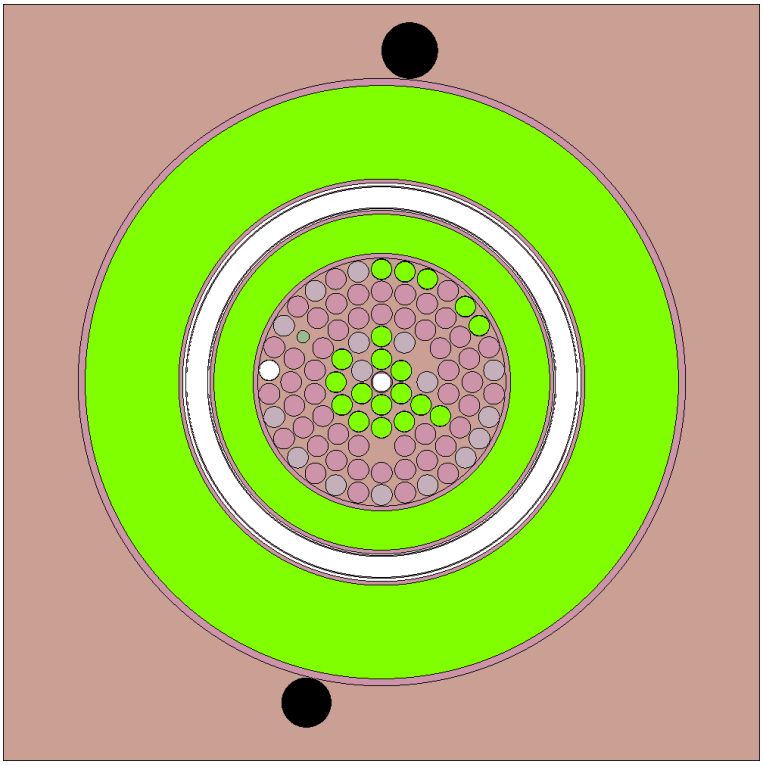

Figure 2.2: TRIGA Mark II Pavia experimental scheme where fuel and control rods concur with the Fig. 2.1. There are the neutron detectors in the ex-core positions in black colour. The detector in the upper part is the ionization chamber (then denoted as number 2) and the detector in the lower part is the fission chamber (then denoted as number 1). The scheme has been retrieved from the Serpent2 model.

TRIGA Mark II Pavia nuclear reactor Serpent2 model

The Serpent2 model for the purposes of the thesis was provided by the professors from Politecnico di Milano. The model was created in 2018 as the topic of the diploma thesis [36] to represent the state of the reactor in 2013. The main problem of the creation of the model was the unknown burn-up of the fuel elements caused during the operation at the high powers (up to 250 kW). The depletion data for the Serpent2 input file were taken from the PhD thesis [37] where the burn-up was calculated in MCNP by dividing the 48 years of reactor operation (1965 to 2013) into 27 time slots. The operating time and various core configurations were combined together with the information about the neutron fluxes derived from the MCNP simulations and then the fuel composition was computed.

The Serpent2 input file from [36] contains two fuel rod types (101 and 103), depleted materials until 2013 and the reactor geometry. Author of this diploma thesis made several changes in the geometry of the control rods and adjusted control rods according to the personal communication with TRIGA Mark II Pavia workers. The lengths of the rods were adjusted to their real value (38.1 cm, respectively, 47.2 cm) and their bottom end position (0 cm) was adjusted according to the personal communication. The bottom end position in the Serpent2 model was set so that the

graphite ending of the control rod is in the same plane as the bottom part of the cladding of the fuel element type 103. From now on, all the rods positions in the text in centimeters are with respect to the bottom part of the cladding of the fuel element type 103. Rods position can be observed at the example of Shim rod in the reactor in Fig.: 2.3.

The author must have added the RaBe neutron source in the axial center of the channel F-4. Moreover, the emission spectrum must have been added to the Serpent2 model. The RaBe neutron source spectrum in the tabular form is unavailable in any open source literature and neither was provided by the workers of the Pavia nuclear reactor. That is why the author approximated the RaBe neutron source with the available experimental AmBe energy spectrum. From the available neutron spectra, the AmBe spectrum has the most similar functional shapes of neutron flux as the RaBe neutron source [38] (see the attached neutron spectra in the appendix B.1). Then the neutron detectors must have been modelled in the ex-core positions and the thermal scattering data must have been added for hydrogen in the ZrH compound. Thermal scattering data for zirconium isotopes in ZrH compound were not used in all calculations due to the very high memory demand. The k-eigenvalue calculations of the TRIGA Mark II model confirmed that the thermal scattering on zirconium isotopes of zirconium in ZrH compound can be neglected since the k_{eff} values concurred within the k_{eff} 1-sigma range, in reactivity units the difference in reactivity between two calculations was -22.3 $\pm$ 37.1 pcm.

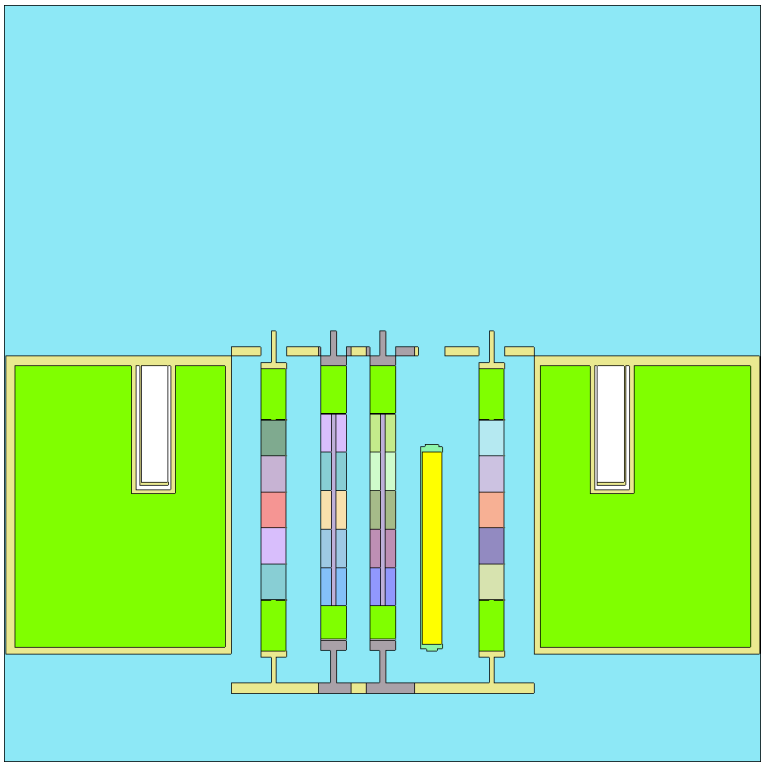

Figure 2.3: TRIGA Mark II Pavia experimental scheme from the side with Shim control rod (yellow). Active fuel part initiates where the colour changes from green. Different colours of the fuel fit the different composition of the fuel during the history of the burn-up.

Moreover, the neutron detectors used during the experiment were included in Serpent2 model. According to some available documentation and observations during the experiment, the beginning of the active length of the ionisation chamber was put 8.25 cm above the ending of the active length of the fuel type 103. According to [35] the active length was set to 8.6 cm and the radius of the cylinder was set to 5.08 cm. During the calculations with the external neutron source, the reaction rate of (n,α) on ^{10}B was being monitored in the volume of the cylinder. The bottom part of the fission chamber was placed according to [35] 1.35 cm above the ending of the active part of fuel type 103. Its active length was set to 20.2 cm with radius 4.495 cm. Similarly, in the active volume of the detector, the reaction rate of total fission on ^{235}U was being followed. The cladding was not modelled for neither of the used detectors.

The Serpent2 model was tested on the data of the zero-power critical states. The value from the forward delayed neutron parameters analogue estimator in Serpent2 calculation of β_{eff} is 653.4 pcm, detailed values of delayed neutron parameters for 6 group division are in Tab. A.1. The results of the reactivity computed from Serpent2 for zero-power critical states are displayed in Tab.: 2.1.

All calculations were performed with version Serpent2.1.32 with nuclear data from the nuclear library ENDF/B-VIII.0.

Table 2.1: Zero-power critical rods positions and the reactivity calculation results of the critical states from Serpent2

Shim position [cm]	Regulating position [cm]	Transient position [cm]	Serpent 2 Reactivity [β_{eff}]
20.0	14.8	47.2	-0.37 $\pm$ 0.02
13.62	38.1	47.2	0.24 $\pm$ 0.02

Results of the Modified Source Multiplication method application in TRIGA Mark II Pavia reactor

Modified Source Multiplication method has been performed in TRIGA Mark II Pavia nuclear reactor in the core configuration from July 2013 (see Fig. 2.1) and this section summarizes the important results of the measurement. The results were obtained for two detector positions corresponding to the scheme in Fig: 2.2. There were detector responses for 13 steady-subcritical states measured, one of them was the reference state. The control rods positions together with reactivity determined from Serpent2 for the subcritical states are displayed in Tab.: 2.2.

The statistical uncertainty following the symbol "$\pm$" not only in this section but in the entire diploma thesis is the standard deviation 1-sigma meaning that 68 % of the values drawn from the normal distribution are within one standard deviation

1-sigma away from the mean value[1]. All the measured and computed values are considered as normally distributed.

Table 2.2: Rods positions during the experiment together with the reactivity determined from Serpent2 in the model mentioned above

Subcritical state	Shim	Regulating	Transient	ρ_S [β_{eff}]
1	down	down	down	-3.71 ± 0.13
2	down	up	down	-2.38 ± 0.08
3	7.57	up	down	-2.63 ± 0.09
4	10.81	up	down	-2.59 ± 0.09
5	down	15.55	down	-3.71 ± 0.13
6	down	26.58	down	-3.07 ± 0.11
7	13.51	up	down	-2.50 ± 0.09
8	16.21	up	down	-2.25 ± 0.08
9	18.37	up	down	-2.07 ± 0.07
10	23.24	up	down	-1.45 ± 0.05
11	25.40	up	down	-1.13 ± 0.04
12	28.10	up	down	-0.71 ± 0.03
ref	13.62	down	up	-0.91 ± 0.03

In order to perform MSM as described in section 1.2, one needs to obtain the detector responses at least from two arbitrary reactor positions, moreover compute the reactivity value from computational code of the reactor together with reaction rates or any similar quantity that is proportional to the detector response. The spatial effect of reactivity is then corrected according to the correction factors in 2.1. It is very important to determine the reactivity in the reference state and measure the detector response in this steady-subcritical state.

$$\frac{\rho_{m,i}(\vec{r}_d)}{\rho_{m,ref(\vec{r}_d)}} = f_{MSM}(\vec{r}_d)\frac{N_{m,ref}(\vec{r}_d)}{N_{m,i}(\vec{r}_d)} = \frac{\rho_{c,i}}{\rho_{c,ref}}\frac{N_{c,i}(\vec{r}_d)}{N_{c,ref}(\vec{r}_d)}\frac{N_{m,ref}(\vec{r}_d)}{N_{m,i}(\vec{r}_d)} \tag{2.1}$$

During the experiment, various steady-subcritical states were reached for about 200 or 300 seconds to measure count rates or voltage respectively in the neutron detectors. The subcritical states are displayed in Tab.: 2.2, where the state "ref" is the reference state.

The reference state was chosen because the reactivity should have met the Regulating rod reactivity worth. The Rod-Drop measurement of reactivity for Transient rod was performed in order to obtain the reference reactivity state. In 2015 during Regulating control rod reactivity worth measurement by reactor period method, 1.41 β_{eff} reactivity worth was obtained [39] (actually 1.26 β_{eff} was obtained during

[1]The propagation of the uncertainties of function $z = f(x_1, x_2, ..., x_n)$ is calculated according to $\sigma_z = \sqrt{\sum_{i=1}^{n}\left(\frac{\partial f}{\partial x_i}\sigma_{x_i}\right)^2}$

the measurement, but in the measurement $\beta_{eff} = 730$ pcm was used, the value of control rod worth was recalculated with respect to the β_{eff} value obtained from the Serpent2 calculation). That could have been the reference value if the measurement was correct. During the experiment the zero power critical state with Regulating control rod in the upper position was reached. Transient rod was also in the upper position, and Shim was in 13.62 cm. The criticality calculation was also performed in Serpent2 for this zero-power critical state, the reactivity value was calculated to 0.24 ± 0.02 β_{eff}.

Rod-Drop reactivity derived from one point kinetic model is determined according to the equation 2.2 [40]. The average count rate value from the fission chamber n_0 was measured for 300 seconds. The sum of delayed neutron properties in 2.2 has been obtained from the Serpent2 criticality calculation. Finally the integral in the denominator was approximated during the measurement by the sum of count rates from the moment of the control rod insertion up to 180 seconds. The total sum was obtained from the counter connected to the fission chamber. It must be mentioned that the counter was activated manually and the author set the time of 180 seconds according to the previous experience. There could have not been obtained any digital results to observe the exponential decrease of the count rates after the rod insertion and so to set precisely the indicator when the rod was dropped and when only background was measured. Once again, it has been demonstrated that reactivity determination is a very difficult subject as the reactivity differs from the Rod-Drop measurement, Serpent2 criticality calculation and control rod reactivity worth measurement from 2015. The results are demonstrated in Tab.: 2.3. Note that Serpent2 $\Delta\rho$ is the difference between the reactivity result in Serpent2 with Regulating rod fully extracted and the reactivity result with Regulating rod fully inserted in the core.

$$\rho = -\frac{n_0 \left(\sum_{i=1}^{6} \frac{\beta_{eff,i}}{\beta_{eff}\lambda_i} \right)}{\int_0^\infty n(t)dt} \; [\beta_{eff}] \tag{2.2}$$

Table 2.3: Value of reactivity in β_{eff} of the MSM reference subcritical state according to the method of determination

Serpent2 $\Delta\rho$	CR reactivity worth [39]	Rod-drop
-1.15 ± 0.04	-1.41	-1.01 ± 0.02

The Source-Jerk measurement could not have been performed because of the reactor scram after removal of the neutron source. In that case, neutron detectors in ex-core positions do not detect the source level, and due to safety requirements, the reactor must be shut down.

The reactivity was measured in two ex-core positions of the neutron detectors. In the following tables, the detector with number 1 is the fission chamber, and the detector denoted as number 2 is the linear ionisation chamber described in the previous section. Tab.: 2.4 sums up the application of the MSM together with "classical"

Source Multiplication (SM) method in order to observe the results of the spatial corrections. There is a reactivity computed from the Serpent2 code of the TRIGA Mark II Pavia model in the last column of the table.

Table 2.4: Reactivity determined by Modified Source Multiplication and Source Multiplication method depending on the position of the detector in the reactor core

	MSM		SM		Serpent2
Subcritical state	$\rho_{m,1}$ $[\beta_{eff}]$	$\rho_{m,2}$ $[\beta_{eff}]$	$\rho_{m,1}$ $[\beta_{eff}]$	$\rho_{m,2}$ $[\beta_{eff}]$	ρ_S $[\beta_{eff}]$
1	-4.50 ± 0.28	-3.41 ± 0.27	-4.27 ± 0.14	-2.06 ± 0.06	-3.71 ± 0.13
2	-2.98 ± 0.18	-2.61 ± 0.20	-2.92 ± 0.09	-1.80 ± 0.05	-2.38 ± 0.08
3	-2.66 ± 0.16	-2.53 ± 0.19	-2.63 ± 0.07	-1.71 ± 0.05	-2.63 ± 0.09
4	-2.30 ± 0.13	-2.33 ± 0.17	-2.27 ± 0.06	-1.59 ± 0.04	-2.59 ± 0.09
5	-3.84 ± 0.23	-3.23 ± 0.25	-3.66 ± 0.12	-1.98 ± 0.06	-3.71 ± 0.13
6	-3.41 ± 0.21	-2.86 ± 0.22	-3.31 ± 0.10	-1.85 ± 0.05	-3.07 ± 0.11
7	-2.07 ± 0.12	-2.18 ± 0.16	-2.01 ± 0.06	-1.49 ± 0.04	-2.50 ± 0.09
8	-1.68 ± 0.10	-1.92 ± 0.14	-1.67 ± 0.04	-1.36 ± 0.03	-2.25 ± 0.08
9	-1.47 ± 0.09	-1.72 ± 0.13	-1.45 ± 0.04	-1.24 ± 0.03	-2.07 ± 0.07
10	-0.92 ± 0.05	-1.18 ± 0.09	-0.90 ± 0.02	-0.89 ± 0.02	-1.45 ± 0.05
11	-0.66 ± 0.04	-0.90 ± 0.07	-0.65 ± 0.02	-0.72 ± 0.02	-1.13 ± 0.04
12	-0.38 ± 0.02	-0.59 ± 0.04	-0.40 ± 0.01	-0.51 ± 0.01	-0.71 ± 0.03

One could consider reactivity results from Serpent2 calculations as the reference value. That is why Tab.: 2.5 is displayed below in order to compare the difference in reactivity determination between reactivity determination methods and Serpent2 results. The difference is calculated from the equation 2.4, where $i = 1, 2$. One can also compare the detector position in the accuracy of determining the reactivity. The results in bold font are the one where the absolute value of the difference is lower for a given detector comparing MSM and SM methods. The discussion of the Serpent2 model together with results is discussed in the following section.

$$\Delta\rho_{m,i} = \rho_{m,i} - \rho_S \tag{2.3}$$

$$\Delta\rho_m = \rho_{m,1} - \rho_{m,2} \tag{2.4}$$

Table 2.5: Reactivity difference according to the equation 2.4 between MSM or SM method and Serpent2 calculation

	MSM		SM	
Subcritical state	$\Delta\rho_{m,1}$ [β_{eff}]	$\Delta\rho_{m,2}$ [β_{eff}]	$\Delta\rho_{m,1}$ [β_{eff}]	$\Delta\rho_{m,2}$ [β_{eff}]
1	-0.79 ± 0.31	**0.30 ± 0.30**	**-0.56 ± 0.19**	1.65 ± 0.15
2	-0.60 ± 0.20	**-0.23 ± 0.22**	**-0.54 ± 0.12**	0.58 ± 0.10
3	-0.03 ± 0.18	**0.10 ± 0.21**	**0.01 ± 0.12**	0.92 ± 0.11
4	**0.29 ± 0.16**	**0.26 ± 0.20**	0.32 ± 0.11	1.00 ± 0.10
5	-0.13 ± 0.27	**0.48 ± 0.28**	**0.05 ± 0.18**	1.73 ± 0.14
6	-0.34 ± 0.23	**0.22 ± 0.25**	**-0.24 ± 0.15**	1.23 ± 0.12
7	**0.43 ± 0.15**	**0.32 ± 0.19**	0.49 ± 0.10	1.01 ± 0.10
8	**0.57 ± 0.13**	**0.33 ± 0.16**	0.58 ± 0.09	0.88 ± 0.09
9	**0.60 ± 0.11**	**0.36 ± 0.15**	0.62 ± 0.08	0.83 ± 0.08
10	**0.53 ± 0.08**	**0.28 ± 0.10**	0.55 ± 0.06	0.56 ± 0.06
11	**0.47 ± 0.06**	**0.23 ± 0.08**	0.48 ± 0.05	0.42 ± 0.05
12	0.32 ± 0.04	**0.12 ± 0.05**	**0.31 ± 0.03**	0.20 ± 0.03

Another way to compare the performance of MSM and SM methods is to compute the difference between the reactivity computed by detector 1 and 2 from the simple equation 2.4. The spatial correction would be fully resolved in the case where the difference would be 0 for each subcritical state. The results of Tab.: 2.6 are also discussed in the following section. The MSM and SM methods are compared, and the bold values in the table are the ones where the absolute value of the difference is lower.

Table 2.6: Reactivity difference between the value determined in position 1 and 2 and its comparison for MSM and SM methods

	MSM	SM
Subcritical state	$\Delta\rho_m$ [β_{eff}]	$\Delta\rho_m$ [β_{eff}]
1	**-1.09 ± 0.39**	-2.21 ± 0.16
2	**-0.37 ± 0.27**	-1.12 ± 0.10
3	**-0.13 ± 0.25**	-0.92 ± 0.08
4	**0.03 ± 0.22**	-0.67 ± 0.07
5	**-0.61 ± 0.34**	-1.68 ± 0.13
6	**-0.55 ± 0.30**	-1.46 ± 0.12
7	**0.10 ± 0.20**	-0.52 ± 0.07
8	**0.24 ± 0.17**	-0.30 ± 0.06
9	0.24 ± 0.15	**-0.21 ± 0.05**
10	0.26 ± 0.10	**-0.01 ± 0.03**
11	0.24 ± 0.08	**0.06 ± 0.02**
12	0.20 ± 0.05	**0.11 ± 0.01**

Discussion of the results of MSM application in TRIGA Mark II Pavia reactor

This section presents a discussion of the results of MSM application in the TRIGA Mark II Pavia reactor. The obtained results from the experiment and the post-processed calculations were the topic of the previous section.

Firstly, the Serpent2 model should be discussed. There have been made several geometric changes in the control rod lengths and bottom end positions according to the personal communication and [33] as described in the section of the Serpent2 model (see Fig.: 2.3, where Shim rod is in the bottom end position). Another issue in TRIGA Mark II Pavia input is that the average fuel composition corresponds to year 2013. The fuel has surely undergone more depletion in the last nine years, nevertheless finding the real fuel composition would be out of the subject of this diploma thesis. The fuel depletion in the last 9 years was not taken into account. It should also be noted that the detector positions were approximated according to the reactor documentation. Moreover, the RaBe neutron spectrum was approximated by AmBe neutron spectrum, the mentioned approximation is mainly significant in the deep subcriticalities as the neutron source spectrum has an impact on how many neutrons are directly emitted from the source. To validate the Serpent2 model, the criticality calculation was performed according to the control rods positions provided from the workers of the nuclear reactor. The zero-power critical state was calculated to -0.37 $\pm$ 0.02 β_{eff}. There was another reactivity of the critical state computed in Serpent2 (0.24 $\pm$ 0.02 β_{eff}), in the other case it was for the critical state from which Rod-Drop measurement was performed. The reactivity value for the critical state different from zero within the uncertainty range is given mainly by the approximated fuel composition (division of the fuel in five axial sections that undergo the depletion, also approximation of the reactor power for the 48 years of reaction operation) and by the bottom end position of the control rods that could be actually slightly different. The fact that the bottom end positions could be different can be observed in the Tab.: 2.2 for the subcritical state 2 and 3. The difference between the subcritical states is that Shim rod is withdrawn by 7.57 cm but in fact Serpent2 calculates the reactivity of the deeper subcritical state 0.25 $\pm$ 0.12 β_{eff} higher. Similarly, the reactivity values for subcritical states 1 and 5 are within the statistical uncertainty even though the Regulating rod (with the lowest reactivity worth) is 15.55 cm withdrawn. It could be a topic of another research work why Serpent2 model calculates higher reactivity for the subcritical state that is deeper then the other one. The author suggests that the reactivity worth in the bottom part of the control rod is so small that statistics cannot catch the small difference and the computed reactivity values are then in two-sigma range. Physically, it can be the graphite inserted as the moderator from the bottom part of the control rod into the plane of active fuel, and then the graphite would aid in moderating the neutrons arriving into other fuel elements. This paragraph should conclude that there is a not negligible systematic uncertainty in the MSM results given by the model of TRIGA Mark II Pavia Serpent2 reactor model higher then the statistic uncertainty.

Secondly, uncertainties given from the experimental measurement should be also discussed. There have been two neutron detectors used for the experiment. The

detectors work in direct current power range mode. No document illustrating the gamma and neutron ratio of detection was available for evaluating the measurement results. Gamma rays can play a non-negligible role in the subcritical reactor with very high contribution to the measured current in the very deep subcritical states. As the neutron flux distribution in different subcritical states strongly depends on the non-linear changes of the neutron flux when changing the reactivity, the measurement requires precise positions of the neutron detectors. Due to the lack of documentation, the position of the neutron detectors was only approximated in the range of more or less 5 cm. Moreover, the voltage from the linear chamber was recorded only on the graph paper during the operation. The experiment requires the digital form of the data as the voltage from the linear chamber read from the graph paper probably includes a systematic error, the statistical error was only approximated graphically. The chamber according to the reactor documentation was considered to work in a linear regime, as its name suggests. On the other hand, the behaviour of the chamber could change during the operation and during various subcritical states. Lastly, it should be also mentioned that the experiment was performed several days after high power operation in order to avoid the poisoning of the reactor. To sum up, it is mainly the elder reactor data acquisition system that inserts a non-negligible uncertainty in the measurement and MSM results.

Taking into account the main systematic uncertainties from Serpent2 and detectors, the results from the previous section could be discussed. It is worthy to debate on the results from Tab.: 2.3 not only in the case of the experiment. The mentioned table proves that determining reactivity in a subcritical state is a very complex problem. Subcritical reactivity can be measured or computed. Considering a measurement, independently of the reactivity determination method, the reactivity value always depends on the position of the detector and in each position of the reactor one would measure a slightly or highly different reactivity value as all the conventional reactivity methods are based on the point kinetics (or any other physical theory) that is only an approximation. Even in the case of the Modified Source Method, the reactivity measurement position will always play a role as the method only modifies by the correction factor (usually computed from MC code) the reactivity values determined by a method based usually on point kinetics (or any other physical approximation). For the calculations, the main issue is the confidentiality of the calculations. The computational model can be verified experimentally on the critical states of the reactors that are demonstrated, for instance, by quasi-constant neutron population when the neutron source is withdrawn from the reactor core or by constant fuel and moderator temperature that is warmer than in the subcritical states. On the other hand, value of the reactivity of the subcritical states cannot be verified on any physical effect and even in the simplest reactors cores, analytical solution cannot be performed. Even though computational codes, especially Monte Carlo codes are considered highly confidential as they perform all the physical processes calculated by the statistical approach. That is why the Monte Carlo codes can be used as a reference but one should be cautious about making conclusions as it is the user who creates the reactor model (that can be different from reality), chooses the nuclear libraries and sets calculation parameters. All of the discussed in this paragraph can be observed in Tab.: 2.3 where Rod-Drop is compared with CR reactivity worth that

was obtained by measuring the reactor period in each supercritical state. Reactivity determined by Rod-Drop of Regulating control rod is 0.10 ± 0.03 different from the reference Serpent2 calculation. The highest uncertainty during the experiment was in measuring the integral in the denominator of the equation 2.2. The only possibility was to get the counts for a chosen interval of time for the fission chamber. The counter was initiated manually when the rod was dropped into the core. The time of the measurement was chosen by the author to be 180 s according to the previous experience in order to avoid summing only the neutron background after the given time. There are two issues when assessing the Rod-Drop measurement, the first one is that the gamma rays contribution to the detector count rate is unknown. The second issue is connected to the fact that the neutron source cannot be withdrawn from the reactor core and that is in contradiction the with the assumptions of the Rod-Drop derivation from point kinetics equations. In theory, it is assumed that the neutron flux would decrease to zero in the subcritical reactor without the neutron source. On the other hand, during the experiment the neutron count rates could have decreased only to the value of 31 cps, which is the value of the neutron count rate measured with the Regulating rod inserted in the reactor. The systematic uncertainty given by the time of the Rod-Drop measurement can be assessed by observing the integral of the count rates and comparing them to the count rates that are given for every second by the subcritical state (Regulating rod inserted). Then the systematic uncertainty of the Rod-Drop measurement would be about 15.5 % as in every second, 31 cps contributed from the subcritical state (5580 counts for 180 s) to the sum and the sum of all the count rates during the Rod Drop was 35 972 cps. The reactivities determined by Serpent2 (the difference between reactivity values with Regulating rod fully withdrawn and fully inserted) and Rod-Drop are in a reasonable interval of concurrence when considering the systematic error of 15.5 %. On the other hand, Rod-Drop measurement and Serpent2 determination are far from the CR reactivity worth determined by the reactor period method.

Regarding the application of MSM method, deciding if the method brings any improvement compared to the SM method, one could focus on decreasing the reactivity difference between two positions of the nuclear reactor or on the determination of the difference between the reactivity in one position and Serpent2 calculation. To check the first criterion, one could discuss the results from Tab.: 2.6, where for 8 subcritical states the difference is lower for the MSM method than for the SM method. In seven of the cases the difference is out of 1-sigma uncertainty range in comparison with SM method. Whereas for four subcritical states closer to the critical state the SM method performed better, in 3 of the those cases it was out of 1-sigma uncertainty range. The SM method is derived from one point kinetics, where the main assumption is that the change of the neutron flux between two different subcritical states is constant in every position. As the reactor reaches the critical state, the neutron flux distribution is getting more symmetrical, and that could be the reason why the SM method is sufficient to determine the reactivity in near critical states. On the other hand, MSM proved to lower the differences in comparison with SM in different positions of the measurement for deep subcritical states. The differences were except for one subcritical state lower than -0.65 β_{eff}. To conclude, the MSM method is capable of capturing spatial effects in a deep subcritical states in TRIGA

Mark II Pavia reactor despite the imperfect Serpent2 model and an inadequate data acquisition system for measurement. The reactivity differences in the position of the measurement for near-critical states (about -2.1 β_{eff}) were below a value 0.26 β_{eff} and that could be caused by a systematic error of the Serpent2 model or the measurement. MSM method also brings satisfying results for the two measuring positions in near-subcritical states but it is enough to use SM method in near-critical states in TRIGA Mark II Pavia reactor.

The other difference in the measurement that can be observed is given by the subcritical behaviour of the nuclear reactor. The neutrons in the subcritical reactor are either created from the subcritical multiplication in the core or can occur directly from the neutron source. Note that in the core configuration Fig.: 2.2, the neutron source in position F-4 is very close to the ionisation chamber denoted by detector number 2 and that is why the direct contribution in position 2 is higher than in position 1. On the other hand, the position 1 is far from the neutron source and the direct neutrons from the source arriving into the detector must undergo the path through the whole diameter of the core. It means that there are more neutrons in position 1 from the subcritical multiplication than in position 2. This phenomenon can also play role in the determination of the reactivity by the MSM method.

The other criterion observed is the reactivity difference between reference Serpent2 calculation and MSM or SM method measurement. It is worthy to note that the Serpent2 calculation is taken as a reference but the model is not fully developed as for the two different critical states the reactivity results were -0.37 $\pm$ 0.02 β_{eff} and 0.24 $\pm$ 0.02 β_{eff}. The results are presented in Tab.: 2.5 and one could observe that for the linear ionisation chamber (detector 2), the reactivity difference was lower for all subcritical states when using the MSM method instead of the SM method. For the subcritical state 5 that was discussed before (the reactivity computed from Serpent2 was lower with less absorber in core than in the other subcritical state), the reactivity difference was 0.48 $\pm$ 0.28 β_{eff}. In other cases, the reactivity difference was always lower than 0.36 $\pm$ 0.15 β_{eff}. However, there were six lower reactivity differences for measurements from the fission chamber (detector 1) when using the MSM method and six lower reactivity differences when using the SM method. But it should be noted that all the differences between MSM and SM are in range of 1-sigma uncertainty range. The reactivity differences when using MSM are higher for the fission chamber than for the linear ionisation chamber. To conclude, for the given measurement and given Serpent2 model of the reactor, MSM method performed better than SM method for the position of the linear ionisation chamber. On the other hand, no conclusions can be drawn on reactivity differences between the fission chamber and Serpent2 calculations.

Lastly, the performance of the application of MSM method in TRIGA Mark II reactor can be compared with the performance of the same method at VR-1 reactor at Czech Technical University in Prague. The reactor is briefly described in section 3.3. The following Tab.: 2.7 shows the results from the previous work [2] focused on the MSM method. The table shows the reactivity determined by MSM method at four positions of detectors and a reactivity difference for three positions in each subcritical state with respect to an arbitrary chosen detector position PMV3. The

reactor VR-1 is very well described in terms of details in Serpent2 model and also in terms of geometries and positions of detectors near the core. One can notice that the differences are in all cases near 0 β_{eff} in the 1-sigma range. The reactivity differences can be compared with MSM performance at TRIGA Mark II reactor in Tab.: 2.6. In case of TRIGA Mark II reactor, the reactivity differences were in all subcritical states higher and out of 1-sigma range than in case of VR-1 reactor. This comparison proves that a MSM method can work with very high precision in a well described reactor in terms of calculation model, reactor geometry and an appropriate data acquisition system.

Table 2.7: Performance of the MSM method in the VR-1 reactor at the Czech Technical University in Prague. Reactivity determined at four positions of detectors and their difference with respect to an arbitrary chosen detector PMV3. A reference reactivity was determined by Source-Jerk method. Results taken from previous work [2].

Detector	PMV1	PMV2	PMV3	PMV4	PMV1	PMV2	PMV4
Subcrit. state	$\rho_{m,1}$ [β_{eff}]	$\rho_{m,2}$ [β_{eff}]	$\rho_{m,3}$ [β_{eff}]	$\rho_{m,4}$ [β_{eff}]	$\Delta\rho_{m,1}$ [β_{eff}]	$\Delta\rho_{m,2}$ [β_{eff}]	$\Delta\rho_{m,4}$ [β_{eff}]
1	-7.91 ± 0.18	-7.90 ± 0.18	-7.91 ± 0.18	-7.89 ± 0.18	0.00 ± 0.25	0.01 ± 0.25	0.02 ± 0.25
2	-7.39 ± 0.17	-7.20 ± 0.16	-7.17 ± 0.16	-7.04 ± 0.16	-0.22 ± 0.23	-0.03 ± 0.23	0.12 ± 0.22
3	-6.28 ± 0.14	-6.06 ± 0.14	-6.09 ± 0.14	-6.02 ± 0.13	-0.19 ± 0.20	0.04 ± 0.19	0.08 ± 0.19
4	-5.84 ± 0.13	-5.65 ± 0.13	-5.64 ± 0.13	-5.51 ± 0.12	-0.19 ± 0.18	-0.01 ± 0.18	0.13 ± 0.18
5	-5.50 ± 0.12	-5.40 ± 0.12	-5.50 ± 0.12	-5.36 ± 0.12	0.00 ± 0.17	0.10 ± 0.17	0.14 ± 0.17
6	-4.70 ± 0.11	-4.57 ± 0.10	-4.59 ± 0.10	-4.61 ± 0.10	-0.11 ± 0.15	0.02 ± 0.15	-0.02 ± 0.15
7	-4.13 ± 0.09	-4.02 ± 0.09	-3.98 ± 0.09	-3.97 ± 0.09	-0.15 ± 0.13	-0.04 ± 0.13	0.00 ± 0.13
8	-3.33 ± 0.07	-3.26 ± 0.07	-3.22 ± 0.07	-3.27 ± 0.07	-0.11 ± 0.10	-0.04 ± 0.10	-0.05 ± 0.10
9	-2.06 ± 0.05	-2.02 ± 0.05	-2.00 ± 0.05	-1.98 ± 0.05	-0.05 ± 0.07	-0.02 ± 0.07	0.02 ± 0.06
10	-1.48 ± 0.04	-1.46 ± 0.03	-1.46 ± 0.03	-1.44 ± 0.03	-0.01 ± 0.05	0.00 ± 0.05	0.02 ± 0.05
11	-0.93 ± 0.02	-0.92 ± 0.02	-0.92 ± 0.02	-0.90 ± 0.02	-0.01 ± 0.03	0.00 ± 0.03	0.02 ± 0.03

To sum up the chapter, there was an experiment designed and performed in TRIGA Mark II Pavia reactor. The Serpent2 reactor model was adjusted and tested on the critical states. The results of the MSM and SM methods were evaluated and compared. It was proven that MSM method is able to capture the spatial effects in all subcritical states even though the calculation model is not perfect and the data acquisition system for the measurement is insufficient. If there is research interest in the future to work on MSM method in TRIGA Mark II Pavia, the Serpent2 model should be improved in terms of verifying the control rods geometry and composition of the fuel rods after years of depletion. In addition, an adequate data acquisition system for neutron measurements should be used.

Chapter 3

Artificial Neural Network for online reactivity monitoring

This chapter deals with the application of recurrent Artificial Neural Network (ANN) for online reactivity monitoring. The method general for zero-power nuclear reactors will be introduced, the workflow of the method will be discussed, a brief description of Recurrent Neural Network will follow. After that, the application of the suggested method will be described and the obtained results will be further commented together with a possible space for improvement.

It was discussed in the previous chapter that there is no reactivity measurement that would not be burdened by a physical approximation in the measurement. In other words, spatial effects in subcritical reactivity measurements can never be fully resolved, and each measurement will contain a systematic error based on physical simplifications. That has been motivation for a new approach to use machine learning in order to predict the reactor reactivity not only in subcritical states. The approach is still based on the physical nature of processes and directly takes into account the spatial effects in the subcritical states. More details about motivation for using the ANN and some other applications of ANN in nuclear field are mentioned in section 1.5.

3.1 General method suggested for online reactivity monitoring of zero-power reactors together with its workflow

The suggested method is based on training the ANN on the previous reactor start-ups and their reactivites computed by a pool of calculations in high fidelity Monte Carlo code. Firstly, historical data of the reactor operation must be collected, especially detector count rates (or any equivalent of the reactor power) in various detector positions together with control rods positions. The main idea behind the application of ANN for online reactivity monitoring in zero-power reactor is that one can make use of Monte Carlo calculations that take into account all the physical

processes experiencing in the nuclear reactor and simulate the physics of it, which is not the case of any other reactivity measurement methods mentioned in the first chapter. The reactivity in a zero-power reactor is determined by fuel composition and position in the core, control rods composition and positions, and a moderator. The fuel composition and position are not changing during the operation of zero-power reactor and it is only the control rod position that determines the changes in reactivity during the operation. These changes can be captured in the criticality calculations in Monte Carlo codes.

This method suggests to calculate reactivities of plenty of subcritical states during the transient process as steady-states. In other words, the transient process such as the reactor start-up is divided with the defined time interval into plenty of steady-states. Then the steady-states criticality calculations are run in Monte Carlo code. In order to save computation time, not all steady-states are computed and for the rest of uncomputed steady-states a polynomial fit of reactivity as a function of position of rods is created. The polynomial fit enables to obtain the reactivity (computed from Monte Carlo code) for all collected start-ups. Then the detector count rates (or their equivalent) are connected again together with the reactivity (obtained from the polynomial fit based on Serpent2 calculations), and these data are the input data for the training and testing of ANN. Please, see Fig.: 3.1 where the workflow is sketched. This approach is general for all zero-power reactors and in the following text, the approach will be repeated and explained for the case of VR-1 research nuclear reactor operated by Czech Technical University in Prague.

The suggested method works with the following constrains:

- The position and emission of neutron sources (mainly fixed neutron source) are not changing during the start-up
- There is no neutron absorber such an experimental device or any object that could have an impact on reactivity inserted in the core
- The count rates on the detectors correspond immediately to the reactivity value after its change

The last constraint is also an inherent property of the method, because the method assumes that immediately after the reactivity change, the count rates (that are at the given time connected with reactivity from Serpent2) correspond to the reactivity value. In reality, it takes a time given by subcritical multiplication until the value of count rates stabilizes. On the other hand, the method is trained on past histories and if in the training the corresponding wrong value of count rates is connected to its correct reactivity value, the wrong value of count rates can precisely determine the reactivity that is computed from Serpent2. But in cases of very high or very low speeds of reactivity changes during the start-up, the method can be imprecise due to the problem of not corresponding count rates to their reactivity value given by the delay from subcritical multiplication.

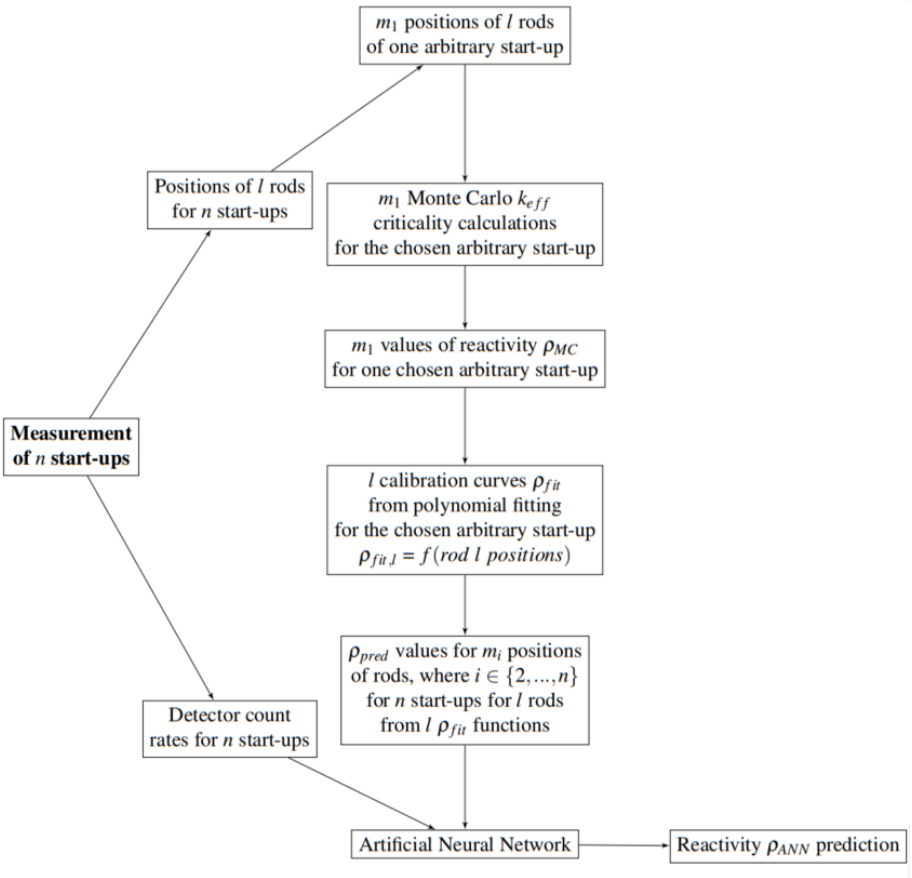

Figure 3.1: Scheme of the workflow to train and test an ANN to predict reactivity. Where l is the number of control rods, n is the number of collected start-ups and m_i is the number of positions of control rods for the i-th start-up.

Once the ANN is trained, tested and validated, it can be used for the purposes of the online reactivity monitoring. It is enough to load the data from the detectors count rates into the ANN as the Fig.: 3.2 shows.

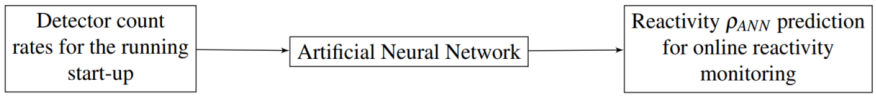

Figure 3.2: Scheme of the online reactivity monitoring by the trained, tested and validated ANN

Due to the nature of the data, the reactor start-ups can be considered as time series for which the application of Recurrent Neural Networks is convenient. That is why a brief introduction into Recurrent Neural Networks will follow.

3.2 Recurrent Neural Networks and their main parameters

The simplest idea behind the ANN is described in section 1.5. Recurrent Neural Network (RNN) has its own specifications, it is a type of ANN that is conveniently used for the data whose input order is important. That is typically the case of time-series data such as the data from the reactor start-up. RNN is the type of a network with feedback and the response at any given time will depend not only on the current input but also on the history of input sequence [24].

Fig.: 3.3 shows a simple explanation of how RNN works. The input layer is denoted as x, h is the recurrent hidden layer, and y is the output layer. The letters A, B, and C represent the network parameters. One can observe that at any given time t, the current input of the hidden layer $h(t)$ is a combination of the input $x(t)$, but also of the previous input of the hidden layer $h(t-1)$. It can be said that the information cycles through a loop to the middle hidden layer. In comparison with the simplest ANN described in section 1.5, the feed-forward (Fig.: 1.3) neural network's output is based only on the current input [41].

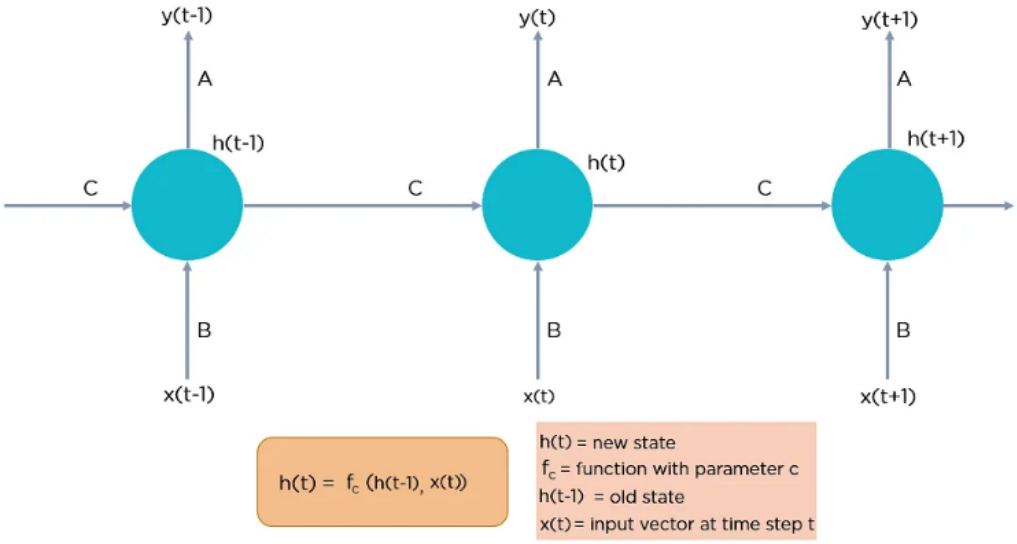

Figure 3.3: Graphical representation of Recurrent Neural Network [41]

In general, there are three types of RNNs: Simple RNN, Long Short-Term Memory (LSTM) RNN and Gated Recurrent Unit (GRU) RNN. Especially the last two have been successfully applied in speech recognition, music synthesis, natural language processing or machine translation [42]. The main advantage of GRU is in gating of network signaling that controls how the present input and previous memory are used to update the current activation and produce the current state. The sets of weights of the gates are adaptively updated in the learning phase, GRU employs only two gate networks [42].

In order to introduce GRU mathematical background, firstly a recurrent hidden

state for simple RNN is presented, corresponding the Fig. 3.3:

$$\vec{h_t} = g(\mathbb{W}\vec{x_t} + \mathbb{U}\vec{h_{t-1}} + \vec{b}) \tag{3.1}$$

where $\vec{x_t}$ is the m-dimensional input vector at time t, $\vec{h_t}$ is the n-dimensional hidden state, g is the activation function (a brief introduction of activation functions will follow), $\mathbb{W}$, $\mathbb{U}$ are $n \times m$ weights and b is an n-dimensional vector of the bias [42]. The equation 3.1 describes how the hidden state vector is computed in the simple RNN as explained above and shown in Fig.: 3.3. Simple RNN has been shown not capable to capture long-term dependencies in the data [42]. That is why, the LSTM and GRU RNNs were developed.

The LSTM RNN gating (control) signals are the input, forget and output, whereas the GRU RNN has only two gates called an update gate $\vec{z_t}$ and a reset gate $\vec{r_t}$ [42]. The function of the update and reset gate is to decide which information should be passed to the output. The gates can keep relevant information to the prediction or remove the irrelevant piece of information. Mathematically, then the hidden state of GRU RNN is presented as:

$$\vec{h_t} = (1 - \vec{z_t}) \odot \vec{h_{t-1}} + \vec{z_t} \odot \vec{\tilde{h}_t}$$
$$\vec{\tilde{h}_t} = g(\mathbb{W}_h\vec{x_t} + \mathbb{U}_h(\vec{r_t} \odot \vec{h_{t-1}}) + \vec{b_h})$$

and the dates operators as:

$$\vec{z_t} = \sigma(\mathbb{W}_z\vec{x_t} + \mathbb{U}_z\vec{h_{t-1}} + \vec{b_z})$$
$$\vec{r_t} = \sigma(\mathbb{W}_r\vec{x_t} + \mathbb{U}_r\vec{h_{t-1}} + \vec{b_r})$$

where σ is the sigmoid function, and similarly $\mathbb{W}_h$, $\mathbb{U}_h$, $\mathbb{W}_z$, $\mathbb{U}_z$, $\mathbb{W}_r$, $\mathbb{U}_r$ are weight matrices and $\vec{b_h}$, $\vec{b_z}$, $\vec{b_r}$ are the bias vectors. Note that $\odot$ stands for the element-wise matrix multiplication [42].

In addition, the role of the activation functions must be explained. In 1989, Cybenko came up with the theorem that any function in interval $[0,1]^n$ can be approximated by a linear combination of sigmoid activation functions [43]. That is in addition to other things the reason why the training and test data must be normalized in the interval [0,1]. Then the Cybenko's theorem was expanded into the Universal approximation theorem that does not specify the activation function only as a sigmoid function. In other words, an ANN consists of multiple layers of neurons that are composed of nodes. Each node has a weight that is considered when processing information in between layers. The activation function aids to detect the non-linear behaviour of the data and physics or nature behind them. The most common activation functions used are: (*i*) binary step function, (*ii*) linear, (*iii*) sigmoid, (*iv*) tanh, (*v*) ReLU„ (*vi*) Leaky ReLU or (*vii*) SoftMax function. If the activation function is not used in an ANN, the output signal would be a simple linear function [44]. That is why

it is very convenient to use activation functions in order to detect the non-linear behaviour of the data.

Among other important parameters in the training phase of the ANN, a loss function must be defined. A loss function controls the deviation between the training data and the ANN output. The loss function must be chosen according to the problem for which the ANN is trained. Examples of the basic loss functions for regression losses are: Mean Squared Error, Mean Absolute Error. The other important parameter for the ANNs is the learning rate. The learning rate or learning coefficient defines how fast the weight of each node is updated in the training process. One of the most widely used methods for weight update is the gradient descent method [43]:

$$w_{j,k}^{t+1} = w_{j,k}^{t} - \eta \frac{\partial E}{\partial w_{j,k}} \tag{3.2}$$

where $w_{j,k}^{t}$ is the weight of the element j, k at time step t of the weight matrix $\mathbb{W}$, E is the loss function and η is the learning rate. The learning rate must be selected in such a way as to find the global minimum of the loss function E. If the learning rate is defined incorrectly, the global minimum of the function E is not reached, and the gradient descent method can remain in the local minimum or simply skip the global minimum if the learning rate is too large and the weights are trained incorrectly [43].

Other important parameters of the ANNs are: optimizer, number of hidden layers, number of nodes in the layer, batch size, percentage of the date used for training.

It is not a trivial task to choose the correct parameters for the ANN. Each data are special and require a different settings of parameters of ANN. The parameters can be found by a method "grid search", when combinations of ANN parameters are put in the large grid and then various ANN are created, trained, validated and tested. Then their performance is evaluated, e.g. by loss and metric functions, and the best ANN is selected.

3.3 Brief description of VR-1 research reactor

VR-1 is a research nuclear reactor operated by Czech Technical University, Faculty of Nuclear Sciences and Physical Engineering, Department of Nuclear Reactors. It is a pool type zero-power nuclear reactor that serves mainly for educational and research purposes. There are four detectors around the core to monitor the power of the reactor (see Fig.: 3.4). Reactivity is controlled usually by six absorption rods of length about 680 mm. There is the IRT-4M nuclear fuel with enrichment of 19.75 % of U-235 in aluminium cladding.

Fig.: 3.4 contains the scheme of core configuration C18 of VR-1 reactor for which the ANN was created. The detectors used for the operational monitoring are marked in green, this configuration contains 6 control rods marked in red.

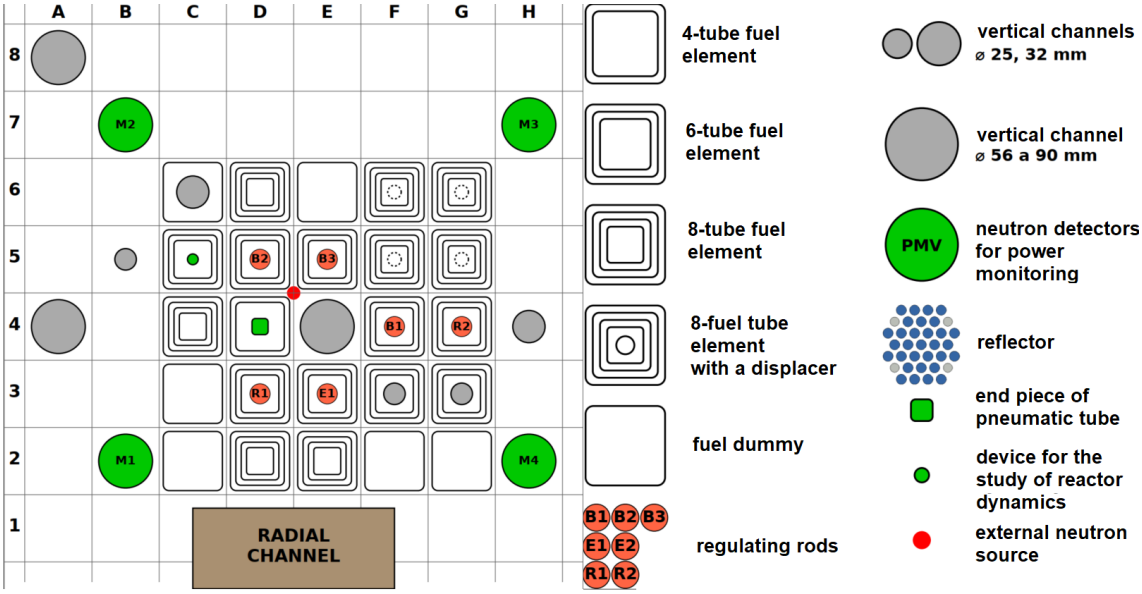

Figure 3.4: The scheme of core configuration C18 for which the ANN was created [45]

3.4 Application of the suggested method in VR-1 research reactor

The suggested method was applied in VR-1 research reactor. The data were collected during the months of operation of the reactor and in total 24 start-ups were used with no experimental devices inserted in the core.

Firstly, the data provided from the start-ups were processed in tabular form such as in the example Tab.: 3.1. Count rates of four detectors used during the operation were collected together with the positions of the control rods each 0.1 second.

Table 3.1: Example of the tabular data from past operation, data are collected every 0.1 second

Detector PMV1 [cps]	Detector PMV2 [cps]	Detector PMV3 [cps]	Detector PMV4 [cps]	Rod B1 [mm]	Rod B2 [mm]	Rod B3 [mm]	Rod E1 [mm]	Rod R1 [mm]	Rod R2 [mm]
...	...	...	...	...	...	...	...	...	...
1572	1551	1647	1464	680.75	681	681.25	335.75	304.25	522.5
1583	1559	1646	1473	680.75	681	681.25	335.75	304.25	523.5
1585	1555	1651	1471	680.75	681	681.25	335.75	304.25	524
1581	1560	1640	1469	680.75	681	681.25	335.75	304.25	524.5
1589	1565	1634	1467	680.75	681	681.25	335.75	304.25	525
1594	1561	1643	1462	680.75	681	681.25	335.75	304.25	525.5
1596	1569	1655	1468	680.75	681	681.25	335.75	304.25	526
...	...	...	...	...	...	...	...	...	...

After the raw data pre-processing, a script was created in order to seize every third combination of the rods position from one arbitrary start-up and the rods positions

were afterwards used as the input data for calculations in Serpent2 code. As one can also notice in Tab.: 3.1, rods position change was usually about $2 \div 3$ millimetres every 0.3 second. Then about 2300 criticality calculations in Serpent2 were run in order to obtain the reactivity in each state of the arbitrary transient process. The computation time for 4 calculations running at the same time on 32 CPUs for each took about 14 days of computation in total.

After the criticality calculations of k_{eff} value were run, a polynomial fit of reactivity for each control rod were created (see Fig.: 3.5). The polynomial fits were created in order to obtain reactivity during the transient process of all start-ups. It is important to mention the fact that the control rods were always withdrawn during the start-up of VR-1 reactor in the same order - first B1, then B2, then B3, then E1, then R1 up to about 303 mm, then R2 and finally R1. This fact was used for the polynomial fitting and the polynomial fits were created for each rod, e.g. B1 in the deepest subcritical states, then B2 and so on. In other words, seven polynomial fits corresponding to six control rods (R1 is withdrawn firstly up to about 303 mm, then R2 is fully withdrawn and then R1 is withdrawn again) were generated. If the rods are withdrawn in an arbitrary order, plenty of combinations of control rods positions could be created, and then a multi-variable polynomial would be created. On the other hand this would rapidly increase the computation time and the hardware demands. For example, if one decides to divide the length of control rods of VR-1 into 10 intervals, he/she would have to run 10^6 calculations to have combination of every possible rods position. In that case, one would run calculations for approximately every 6.8 centimeters change in rods position. Note that the way used for the purposes of the diploma thesis enabled to run calculations for approximately every 2 millimeters change in rods position and moreover only about 2300 calculations were run. What is more, only one variable polynomial could have been generated for every control rod due to the nature of the data from VR-1. An example of the control rods polynomials is presented in Fig.: 3.5. The scripts for the control rods position extraction, the creation of the pool of Serpent2 calculations inputs, and the polynomial fits were performed in Python 3.9.7.

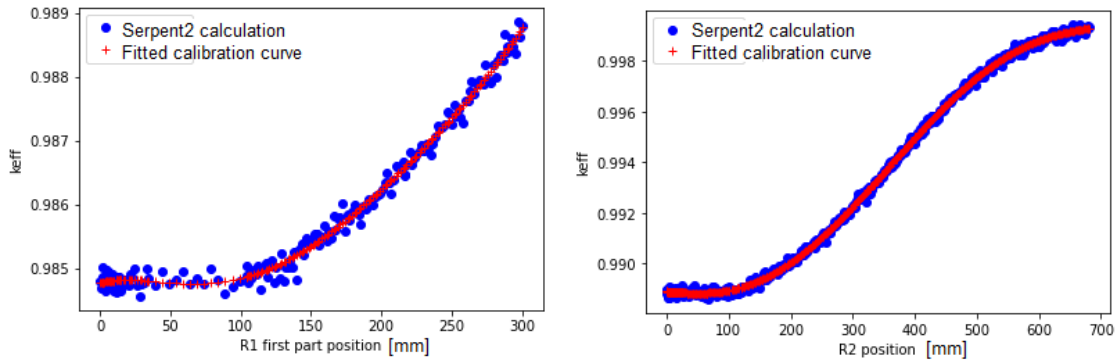

Figure 3.5: Examples of reactivity/k_{eff} polynomial fits for R1 and R2 control rods, data in blue are the results of criticality calculations from Serpent2 and the data in red are polynomial fit approximation of all positions of each control rod during the transient process

Serpent2 model of core configuration C18 of the reactor VR-1

The model of the reactor VR-1 core configuration C18 was provided to the author of the thesis by the Department of Nuclear Reactors, Faculty of Nuclear Sciences and Physical Engineering, Czech Technical University of Prague. It is a standard model used for various types of calculations by a large group of users.

The reactivity of the critical state in the Serpent2 model was validated with the experiment and the results of the reactivity in the official reactor documentation [45] were calculated as ρ_{crit} = -0.012 ± 0.014 β_{eff}. The value of β_{eff} = 7.8869e-03 was taken from the official documentation of the reactor core configuration [45].

The calculations were performed in the version Serpent2.1.32. with nuclear library ENDF/B-VIII.0 in criticality source mode with 60 000 neutrons simulated per generation in 1 500 active generations and 40 inactive generations resulting in k_{eff} standard deviation in range from 0.00011 - 0.00014.

Artificial Neural Network of the VR-1 reactor in Python

In total, 24 historical start-ups in configuration C18 were available, 70 % of them (cca 17 start-ups) were used as the training data, then 10 % of them (cca 3 start-ups) were used for the validation part, and 20 % of them (cca 4 start-ups) were used for the test phase. The training data are the data used for the determination of the ANN weights, the validation data (in some literature called confusingly as tested data) are the data used during the training process in order to evaluate the accuracy of the prediction by following the loss function. That is why the validation data have an indirect impact on the ANN weights. On the other hand, there is also a set of test data that does not have any impact on the ANN and it is never used during the training process. The test data serve to evaluate the model performance once the training phase is finished.

The model of the ANN was created in Python 3.9.7. in Keras Application Programming Interface running on the machine learning platform TensorFlow. It is an open-source machine learning platform developed with a focus on enabling fast experimentation and research [46].

The code of the model itself with its detailed description is a subject of Appendix C. Furthermore, a second code intended to be used for online monitoring based on ANN is in the Appendix D and can be applied in the online monitoring system of not only VR-1 reactor.

In order to find the best fitting parameters of the ANN, in total 24 ANNs were created and evaluated. The table of parameters is presented in Tab.: 3.2. The last ANN was chosen based on the low value of the metric function which was followed during the training. The metric function is a function that evaluates the performance of the ANN and has no impact on the weights in contrary to the loss function discussed in section 3.2. The metric function was chosen as the Mean Absolute Percentage Error (MAPE) and its value converged to $9.7 \cdot 10^{-4}$ %. There was no other reason to look for an ANN with other parameters due to the order of Δk_{eff}

from the Serpent2 calculations between two close subcritical states. For those an absolute percentage error was computed for two different subcritical states differed only by a slight control rod change ($2 \div 3$ mm as shown in Tab. 3.1). In the deepest subcriticalities, the absolute percentage error was $\Delta k_{eff} = 1.8 \cdot 10^{-2}$ % and for the subcriticalities very close to the critical state, the absolute percentage error was $\Delta k_{eff} = 1.7 \cdot 10^{-2}$ %. In other words, the order of precision of the ANN was one order lower than the resolution in between the reactivities of two close subcritical states. A higher resolution could be reached if more neutrons per cycle were generated in Serpent2 calculations, nevertheless, that would cost more computational time.

Table 3.2: Tested parameters of the ANN and their loss and metric functions

ANN number	Recurrent layer model	Optimizer	Optimizer learning rate	Input layer activation function	Number of hidden layers	Hidden layer activation function	Number of nodes in the input layer	Number of nodes in the hidden layer #1	Number of nodes in the hidden layer #2	Output layer activation function	Percentage of data used for training [%]	Loss function after convergence MSE	Metric function after convergence MAPE [%]
1	LSTM	Adam	0.01	tanh	1	tanh	128	128	xxx	sigmoid	70	3.7E-05	2.9E-03
2	LSTM	Adam	0.01	relu	1	relu	128	128	xxx	sigmoid	70	5.1E-05	3.6E-03
3	LSTM	Adam	0.01	relu	0	xxx	128	xxx	xxx	sigmoid	70	6.9E-05	4.1E-03
4	LSTM	Adam	0.01	tanh	0	xxx	128	xxx	xxx	sigmoid	70	2.9E-05	2.5E-03
5	LSTM	Adam	0.01	tanh	1	tanh	64	128	xxx	sigmoid	70	4.0E-05	3.0E-03
6	LSTM	Adam	0.01	tanh	0	xxx	128	xxx	xxx	tanh	70	5.2E-05	3.4E-03
7	LSTM	Adam	0.01	tanh	0	xxx	64	xxx	xxx	sigmoid	70	3.1E-05	2.5E-03
8	LSTM	Adam	0.01	tanh	0	xxx	256	xxx	xxx	sigmoid	70	2.7E-05	2.4E-03
9	LSTM	Adam	0.005	tanh	0	xxx	96	xxx	xxx	sigmoid	70	3.1E-05	2.8E-03
10	LSTM	Adam	0.01	tanh	0	xxx	96	xxx	xxx	sigmoid	70	3.6E-06	1.0E-03
11	LSTM	Adam	0.01	tanh	1	tanh	256	512	xxx	sigmoid	70	1.6E-03	3.3E-02
12	LSTM	Adam	0.01	tanh	0	xxx	512	xxx	xxx	sigmoid	70	7.9E-06	1.5E-03
13	LSTM	Adam	0.01	tanh	0	xxx	256	xxx	xxx	relu	70	9.3E-01	9.7E-01
14	SimpleRNN	Adam	0.01	tanh	0	xxx	96	xxx	xxx	sigmoid	70	7.1E-05	3.6E-03
15	GRU	Adam	0.01	tanh	0	xxx	96	xxx	xxx	sigmoid	70	1.7E-06	9.1E-04
16	LSTM/Dropout	Adam	0.01	tanh	1	xxx	96	xxx	xxx	sigmoid	70	2.7E-05	3.0E-03
17	LSTM	Adam	0.01	tanh	2	tanh	64	96	64	sigmoid	70	4.5E-05	3.0E-03
18	LSTM	Adam	0.01	tanh	1	tanh	96	32	xxx	sigmoid	70	5.2E-05	3.3E-03
19	GRU	Adam	0.01	tanh	0	xxx	128	xxx	xxx	sigmoid	70	1.7E-06	9.2E-04
20	LSTM	Adam	0.01	tanh	0	xxx	512	xxx	xxx	sigmoid	80	8.1E-06	1.5E-03
21	LSTM	Adam	0.01	tanh	0	xxx	512	xxx	xxx	sigmoid	65	1.4E-05	1.8E-03
22	LSTM	Adam	0.01	tanh	0	xxx	720	xxx	xxx	sigmoid	70	7.7E-06	1.4E-03
23	GRU	Adam	0.01	tanh	0	xxx	512	xxx	xxx	sigmoid	70	2.8E-06	9.8E-04
24	**GRU**	**Adam**	**0.01**	**tanh**	**0**	**xxx**	**256**	**xxx**	**xxx**	**sigmoid**	**70**	**2.7E-06**	**9.7E-04**

3.5 Results of the reactivity prediction based on the ANN on VR-1 start-up data and their discussion

The ANN with parameters in bold from Tab.: 3.2 was trained, tested, validated (see the code in Appendix C) and then used on two arbitrary start-up data. The Mean Square Error (MSE) as the loss function converged to $2.7 \cdot 10^{-6}$ and the Mean Absolute Percentage Error (MAPE) converged to the value of $9.7 \cdot 10^{-4}$.

The Fig.: 3.6 and 3.7 show the results of the ANN performance on the arbitrary start-ups data together with the results from the reactimeter implemented in the control system of the reactor based on averaging the detector count rates from four detector positions and then calculating the reactivity by the inverse kinetic equation 1.3. Furthermore, the reactivities for detectors PMV1-4 positions determined by the inverse kinetic equation 1.3 are also displayed. In addition, the polynomial calibration curves of the start-ups on which the ANN was trained are plotted in the graphs. This set of calibration curves is considered as a referring value of reactivities despite the physical problem that the count rates stabilize for a given reactivity after some time given by subcritical multiplication. It can be seen that the calibration curve in the near critical state gives values slightly supercritical which is caused by an inappropriate fit function. Perhaps, a trigonometric function could be used for fitting. One can observe that the ANN is not capable of predicting the reactivity in the deepest subcritical states but on the other hand in Fig.: 3.6 the reactivity determined by ANN from -6 β_{eff} copies the curve of the polynomial and the mean reactivity error in this range is only 2 pcm for the start-up 1. The mean reactivity error[1] with respect to the calibration curves from Serpent2 is displayed in Tab.: 3.3. It can be seen that spatial effects, indeed, play a not negligible role when using the simplified point kinetics model. On the other hand, the point kinetics model was more capable to predict the reactivites in the deepest subcritical states despite very high oscillations of the reactivity value (around 1 β_{eff} in Fig.: 3.6). In the subcritical states near the critical, the ANN performs better than the point kinetics model, mean reactivity error for start-up 1 and start-up 2 was only 2 pcm, respectively 66 pcm.

It must be mentioned that the performance of the reactimeter based on the point kinetics is highly dependent on the source term in equation 1.3. The source level can be tuned in such a way that the point kinetics performs better in subcritical states near the critical state and usually performs worse in the very deep subcritical states, or the source term can be tuned for the deep subcritical states, but then usually the point kinetics performs worse in the subcritical states near the critical.

Researching more appropriate fit functions of reactivity calibration curves could be performed as in Fig.: 3.5, 3.6 and 3.7 was shown that determining the reactivity values on the rods boundaries is a bit problematic for the polynomial function, and

[1]Mean reactivity error was calculated as ME = $\sum_i^n \frac{(\rho_{c,i} - \rho_{fit,i})}{n}$, where $\rho_{c,i}$ is the reactivity calculated by ANN or PK method for time step i, $\rho_{fit,i}$ is the reactivity determined by polynomial fit from Serpent2 and n is the length of time interval

Table 3.3: Comparison of mean reactivity error for ANN and PK for various detector positions, PK stands for inverse point kinetics equation 1.3

	Start-up 1			Start-up 2		
Method	$\Delta\rho$ [pcm]	$\Delta\rho$ [pcm] $\rho > -6\ \beta_{eff}$	$\Delta\rho$ [pcm] $\rho < -6\ \beta_{eff}$	$\Delta\rho$ [pcm]	$\Delta\rho$ [pcm] $\rho > -6\ \beta_{eff}$	$\Delta\rho$ [pcm] $\rho < -6\ \beta_{eff}$
ANN	112	2	467	205	66	754
PK - PMV1-4 average	-107	-118	-69	-72	-113	93
PK - PMV1	-210	-189	-279	-50	-111	195
PK - PMV2	-143	-100	-283	-70	-87	-5
PK - PMV3	-199	-180	-262	-107	-148	52
PK - PMV4	-787	-492	-1745	-483	-330	-1087

perhaps, an appropriate trigonometric function could be used.

It should be stated that the ANN was trained only on 17 start-ups and its performance could get better by collecting more start-up histories. Moreover, the uncertainty from Serpent2 calculations could be lowered by simulating more neutrons per generation. Then even better parameters of the ANN could be found and lowering the Mean Absolute Percentage Error of the model would make sense.

The method itself may not be ideal for reactor VR-1 due to very frequent core changes (annual), but there are zero-power reactors in the world where the core remains the same for decades.

The viability of reactivity monitoring by ANN on a limited domain (order of rods withdrawal, no experimental devices in the core, constant position of neutron sources in time) was proved.

Presently the method is limited by previous operation of the reactor in order to predict the reactivity. An important further improvement of the suggested idea can be done, especially in the part of the detectors response. If one verifies that the detector response is proportional to the computed reaction rates of the detectors from Monte Carlo calculations, a new core loading in the future could be done based only on the ANN. In that case, ANN would be able to connect the change in detector response with change in reactivity. The author of the thesis believes that if further research is conducted, a completely new method for reactivity monitoring could be discovered.

However, it must be stated that the entire method suggested is based on high fidelity of Monte Carlo codes in subcritical states. Furthermore, the Monte Carlo model is always limited by the user who creates the geometry, makes decisions what physics will be simulated and chooses nuclear libraries. That can result in the unknown difference between the real reactivity value and an ANN model prediction. The difference from Serpent2 model can be observed in Fig.: 3.6 when reactor reaches the critical state and the reactivity determined by the polynomial based on Serpent2 is approximately 0.25 β_{eff}.

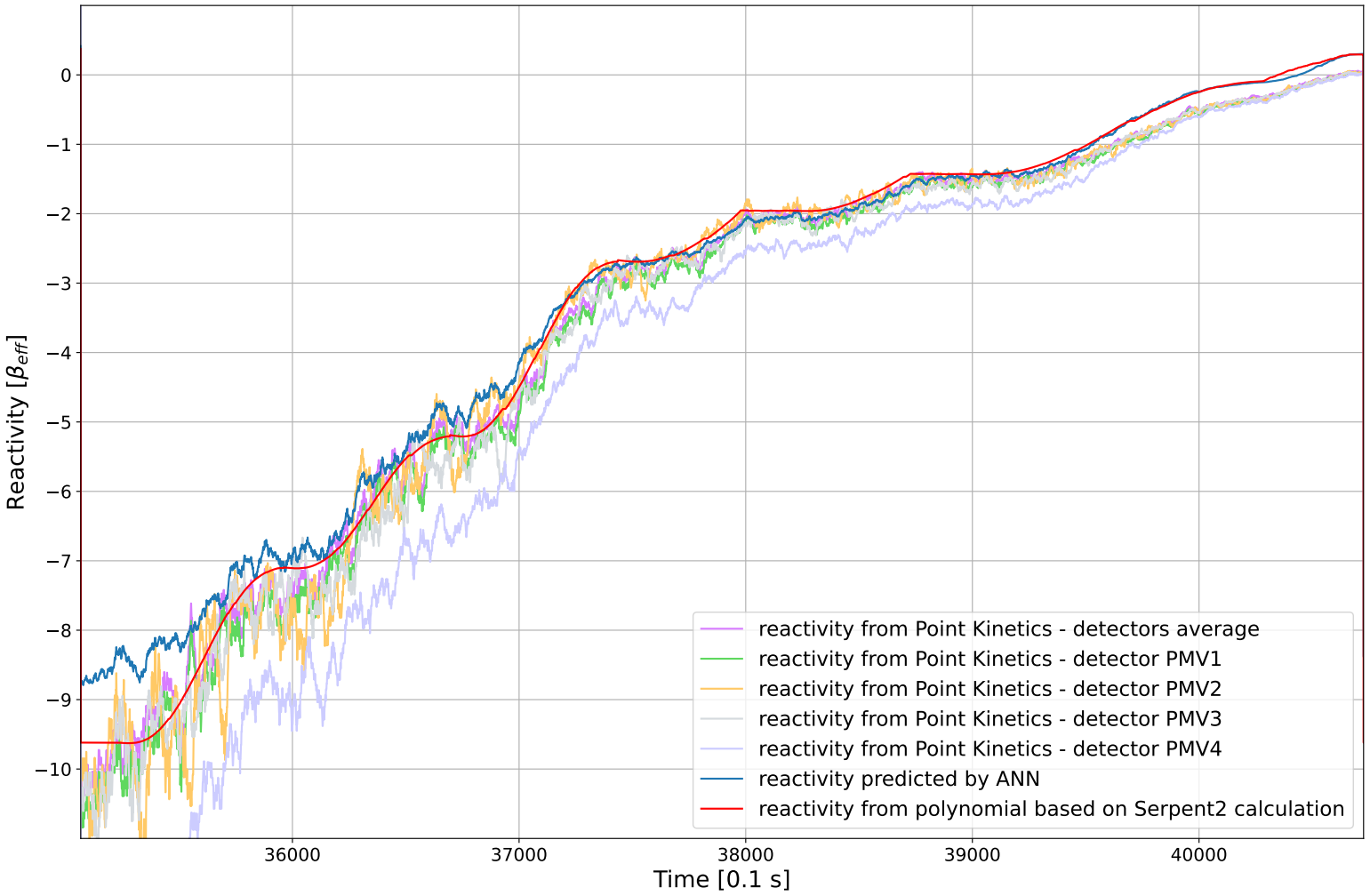

Figure 3.6: Reactivity prediction by ANN, Point Kinetics equation and the polynomial based on Serpent2 calculation for an arbitrary start-up 1. The start on the time axis is from an arbitrary value.

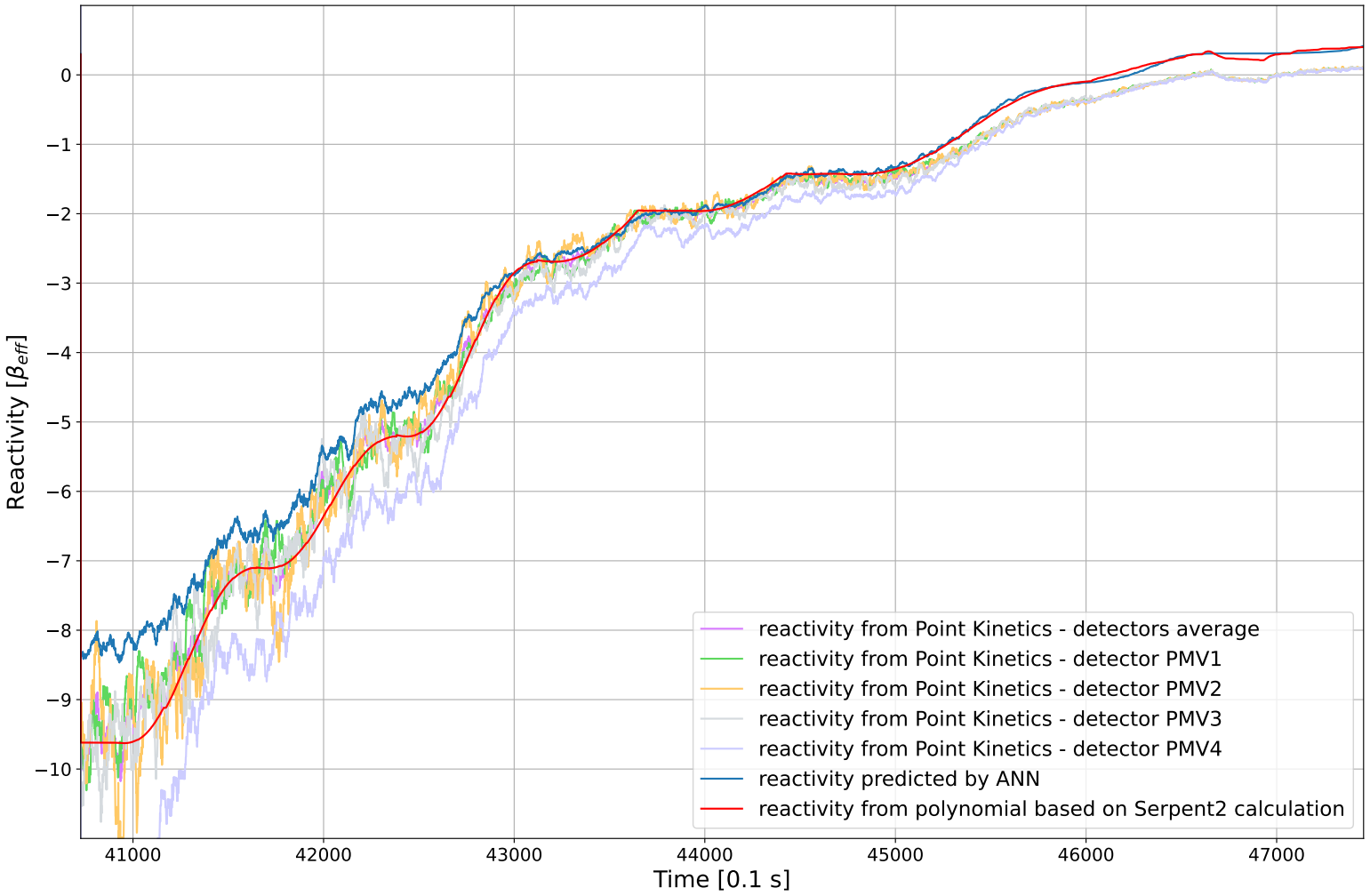

Figure 3.7: Reactivity prediction by ANN, Point Kinetics equation and the polynomial based on Serpent2 calculation for an arbitrary start-up 2. The start on the time axis is from an arbitrary value.

Conclusions

The main aim of the diploma thesis was on the topic of spatial effects in reactivity measurements in subcritical states of research reactors. First of all, a survey of the methods regarding the spatial effects in subcritical states was performed and moreover the methods limitations were discussed. Besides that, a new method for online reactivity monitoring was suggested by the author of the thesis.

One of the methods mentioned in the survey, namely Modified Source Method, was selected for the experiment at TRIGA Mark II reactor in Pavia, Italy. The experiment was designed and performed. Moreover, the results post-processing and discussion of spatial corrections were executed. Modified Source Method proved to be suitable for lowering the spatial effects in reactivity determination in spite of imperfect Serpent2 model of the reactor and an insufficient data acquisition system. Furthermore, improvements for the future experiments regarding Modified Source Method were suggested in the chapter 2. The Modified Source Method at TRIGA Mark II reactor in Pavia was compared with the performance of the same method performed at well physically described reactor VR-1 in Prague (see Tab.: 2.6 and Tab.: 2.7) in previous work [2]. The performed experiment and its results led the author to conclusions that determining the reactivity of a subcritical reactor is a very complex task. On one hand, the reactivity can be measured and on the other hand it can be computed by best-estimate codes. If a measurement is considered, it always takes into account a physical model based on simplifications that must consider spatial corrections if one wants to deal with them. In other words, there is no method that would be able to measure subcritical reactivity regardless of the spatial effects. There are some spatial effects correction factors, but they only complement the methods based on physical assumptions. Alternatively, reactivity can be computed by best-estimate codes, especially by Monte Carlo ones, that are considered as high-fidelity codes as they represent all the physics occurring by a statistical approach. Then what comes to mind is the confidentiality of the calculations as they are still based on a human user who creates the model, chooses nuclear data libraries and selects the simulation parameters. That results in the differences between the reality and the physical model given by the material and geometrical uncertainties. The drawback of the reactivity measurement and calculation is that the subcritical reactivity value cannot be verified on any physical effect or any analytical solution even in the simplest reactors cores.

The previous argumentation led the author to suggest a new method for online reactivity monitoring based on calculations of the subcritical states in Monte Carlo Serpent2 code and following that a creation of an Artificial Neural Network trained

on the past start-up histories of the reactor VR-1 in Prague. The ANN was created in Python, the code of ANN and its usage in online reactivity monitoring are the subjects of the appendix. The method is suitable for online reactivity monitoring of any zero-power reactor. Both codes can be used and employed not only in VR-1 reactor.

In general, the ANN performance proved that Machine Learning could also be used in the nuclear field together with other systems, such as, in this case, the point kinetics reactimeter. Moreover, the diploma thesis showed the viability of reactivity monitoring by ANN on a limited domain (order of rods withdrawal, no experimental devices in the core, constant position of neutron sources in time). The author of the thesis believes that if more start-up data is used in combination with lowering the uncertainty from Serpent2 calculation, ANN could perform with a very high precision. To prove this, further research will be needed. The optimization could be performed for time-step sensitivity of the transient process division; moreover, the dependence of the fit function choice should be monitored, and lastly the method could be applied at other zero-power reactors. Moreover, if the ANN is trained on more reactor start-ups in the future, its performance can be improved. ANN reactivity prediction by ANN was compared with calibration curves for each control rod based on Serpent2 calculations and a point kinetics reactimeter. For reactivites higher then -6 β_{eff} of two arbitrary start-ups, the mean reactivity error of ANN were only 2 pcm, respectively 66 pcm. Especially if computed change in the reaction rates at detectors from Serpent2 code proves to be proportional to the change of the detector response, the ANN method could be used for the reactivity monitoring and new core loading without any previous data collection.

Bibliography

[1] Kladiva, Petr. *Studium podkritického reaktoru s externími zdroji neutronů [Study on subcritical system with external neutron sources].* Bachelor Thesis. Prague. Czech Technical University of Prague, Faculty of Nuclear Sciences and Physical Engineering, Department of Nuclear Reactors. 2020. Supervisor Ing. Tomáš Bílý, Ph.D.

[2] Kladiva, Petr. *Studium prostorových vlivů při stanovení reaktivity aktivní zóny jaderného reaktoru v podkritickém stavu [Study on spatial effects in subcritical reactivity determination in nuclear reactor core].* Year project. Prague. Czech Technical University of Prague, Faculty of Nuclear Sciences and Physical Engineering, Department of Nuclear Reactors. 2021. Supervisor Ing. Tomáš Bílý, Ph.D.

[3] BLAISE, Patrick & MELLIER, Frédéric & FOUGERAS, Philippe. (2009). *Application of the Modified Source Multiplication (MSM) technique to subcritical reactivity worth measurements in thermal and fast reactor systems.* IEEE Transactions on Nuclear Science. 58. 1 - 9. 10.1109/ANIMMA.2009.5503677.

[4] Wang, Wen-Cong & Huang, Li-Yuan & Liu, Cai-Xue & Feng, Han & Niu, Jiang & Dai, Qi-Dong & Fu, Guo-En & Yang, Lin-Feng & Wu, Ming-Chang. (2021). *First application of large reactivity measurement through rod drop based on three-dimensional space–time dynamics.* Nuclear Science and Techniques. 32. 10.1007/s41365-021-00856-4.

[5] Nirmal Kumar Ray, L.M. Pant, Tarun Patel, Rajeev Kumar, Tushar Roy, P.S. Sarkar, Amar Sinha, S.C. Gadkari, *Experimental validation of noise theory developed by considering the source as an exponentially correlated process in D-T neutron generator driven subcritical system*, Progress in Nuclear Energy, Volume 117, 2019, 103087, ISSN 0149-1970, https://doi.org/10.1016/j.pnucene.2019.103087.

[6] HEŘMANSKÝ, B., *Jaderné reaktory [Nuclear Reactors].* Praha: SNTL - Nakladatelství technické literatury, 1981.

[7] Bell, G.I. and Glasstone (1970) *Nuclear Reactor Theory.* Van Nostrand Reinhold Ltd., New York.

[8] Schiassi, Enrico & De Florio, Mario & Ganapol, Barry & Picca, Paolo & Furfaro, Roberto. (2021). *Physics-informed neural networks for the point kinetics equations for nuclear reactor dynamics.* Annals of Nuclear Energy. 108833. 10.1016/j.anucene.2021.108833.

[9] Ganapol, B., Picca, P., Previti, A., & Mostacci, D. (2012). The solution of the point kinetics equations via converged accelerated Taylor series (CATS). In International Conference on the Physics of Reactors 2012, PHYSOR 2012: Advances in Reactor Physics (pp. 3391-3409). (International Conference on the Physics of Reactors 2012, PHYSOR 2012: Advances in Reactor Physics; Vol. 4).

[10] Paolo Picca, Roberto Furfaro, Barry D. Ganapol, A highly accurate technique for the solution of the non-linear point kinetics equations, Annals of Nuclear Energy, Volume 58, 2013, Pages 43-53, ISSN 0306-4549, https://doi.org/10.1016/j.anucene.2013.03.004.

[11] S. J. Julier and J. K. Uhlmann, *Unscented filtering and nonlinear estimation*, in Proceedings of the IEEE, vol. 92, no. 3, pp. 401-422, March 2004, doi: 10.1109/JPROC.2003.823141.

[12] Yamanaka, Masao & Watanabe, Kenichi & Pyeon, Cheol Ho. (2020). *Subcriticality estimation by extended Kalman filter technique in transient experiment with external neutron source at Kyoto University Critical Assembly.* The European Physical Journal Plus. 135. 10.1140/epjp/s13360-020-00270-6.

[13] Dulla, Sandra, P. Ravetto and Paolo Saracco. *Some New Thoughts on the Multipoint Method for Reactor Physics Applications.* M&C 2017 - International Conference on Mathematics & Computational Methods Applied to Nuclear Science & Engineering, Jeju, Korea, April 16-20, 2017.

[14] Jean-Luc Lecouey, Anatoly Kochetkov, Antonin Krása, Peter Baeten, Vicente Bécares, Annick Billebaud, Sébastien Chabod, Thibault Chevret, Xavier Doligez, François-René Lecolley, Grégory Lehaut, Nathalie Marie, Frédéric Mellier, Wim Uyttenhove, David Villamarin, Guido Vittiglio, Jan Wagemans, *Monte Carlo MSM correction factors for control rod worth estimates in subcritical and near-critical fast neutron reactors*, EPJ Nuclear Sci. Technol. 1, 2 (2015)

[15] Guillaume Truchet, W.F.G. van Rooijen, Y. Shimazu, K. Yamaguchi, *Application of the modified neutron source multiplication method to the prototype FBR Monju*, Annals of Nuclear Energy, Volume 51, 2013, Pages 94-106, ISSN 0306-4549, https://doi.org/10.1016/j.anucene.2012.07.040.

[16] Masashi TSUJI , Nobuhide SUZUKI & Yoichiro SHIMAZU (2003) *Subcriticality Measurement by Neutron Source Multiplication Method with a Fundamental Mode Extraction*, Journal of Nuclear Science and Technology, 40:3, 158-169, DOI:10.1080/18811248.2003.9715346

[17] BÍLÝ Tomáš, Jan RATAJ, Petr KLADIVA, Benchmark on neutron flux spatial effects in subcritical system based on IRT-4 M fuel for near-core positions, Annals of Nuclear Energy, Volume 157, 2021, 108231, ISSN 0306-4549, https://doi.org/10.1016/j.anucene.2021.108231.

[18] E. K. Lee, H. C. Shin, S. M. Bae, et al, *Application of the dynamic control rod reactivity measurement method to Korea Standard Nuclear Power Plants.* In: Proceedings of the PHYSOR 2004, Chicago, IL, April 25–29(2004), ANS.

[19] Jaakko Leppänen, Manuele Aufiero, Emil Fridman, Reuven Rachamin, Steven van der Marck, Calculation of effective point kinetics parameters in the Serpent 2 Monte Carlo code, Annals of Nuclear Energy, Volume 65, 2014, Pages 272-279, ISSN 0306-4549, https://doi.org/10.1016/j.anucene.2013.10.032.

[20] Karl O. Ott, Robert J. Neuhold. *Introductory Nuclear Reactor Dynamics.* (American Nuclear Society, Illinois, 1985)

[21] Joon Gi Ahn, Nam Zin Cho & Jung Eui Kuh (1993) *Generation of Spatial Weighting Functions for Ex-Core Detectors by Adjoint Transport Calculation*, Nuclear Technology, 103:1, 114-121, DOI: 10.13182/NT93-A34834

[22] Farkas, Gabriel & Lipka, Jozef & Haščík, Ján & Slugen, Vladimir. (2013). *Computation of ex-core detector weighting functions for VVER-440 using MCNP5.* Nuclear Engineering and Design. 261. 226-231. 10.1016/j.nucengdes.2013.01.026.

[23] C. Berglöf, M. Fernández-Ordóñez, D. Villamarín, V. Bécares, E. M. GonzálezRomero, Victor Bournos, Ivan Serafimovich, Sergei Mazanik & Yurii Fokov (2010). *Spatial and Source Multiplication Effects on the Area Ratio Reactivity Determination Method in a Strongly Heterogeneous Subcritical System*, Nuclear Science and Engineering, 166:2, 134-144, DOI:10.13182/NSE09-87

[24] Hagan, Martin & Demuth, Howard & Beale, Mark & de Jesús, Orlando. 2014. *Neural Network Design (2nd edition).* USA.

[25] M. El-Sefy, A. Yosri, W. El-Dakhakhni, S. Nagasaki, L. Wiebe, *Artificial neural network for predicting nuclear power plant dynamic behaviors*, Nuclear Engineering and Technology, Volume 53, Issue 10, 2021, Pages 3275-3285, ISSN 1738-5733, https://doi.org/10.1016/j.net.2021.05.003.

[26] Pereira Filho, Leonidas, Kelling Cabral Souto, and Marcelo Dornellas Machado. *Using neural networks for prediction of nuclear parameters.* 013 International Nuclear Atlantic Conference - INAC 2013 Recife, PE, Brazil, November 24-29, 2013.

[27] Alexander Nakhabov, Valery Kolesov, Pavel Soglaev, *Prediction of a reactivity margin for partial refueling of nuclear reactor using artificial neural networks*, Procedia Computer Science, Volume 169, 2020, Pages 310-313, ISSN 1877-0509, https://doi.org/10.1016/j.procs.2020.02.188.

[28] J. Ma, J. Fan, L. Lv and L. Ma, *Reactivity estimation of nuclear reactor combined with neural network and mechanism model*, 2012 IEEE Power and Energy Society General Meeting, 2012, pp. 1-6, doi: 10.1109/PESGM.2012.6345243.

[29] Dulla, S., P. Picca, and M. Carta. *Methods for the reactivity evaluation in subcritical systems analysis: a review.* International Conference on Mathematics and Computational Methods Applied to Nuclear Science and Engineering (M&C 2011) Rio de Janeiro, RJ, Brazil, May 8-12, 2011.

[30] Kiedrowski, Brian, and Forrest Brown. *MCNP Calculations of Subcritical Fixed and Fission Multiplication Factors.* San Diego, CA, USA. 2010

[31] Viitanen, T., & Leppaenen, J. Lyoussi, A. (Ed.). (2016). *Validating the Serpent model of FiR 1 Triga Mk-II reactor by means of reactor dosimetry.* France: EDP Sciences.

[32] Sergey V. Bedenko, Gennady N. Vlaskin, Nima Ghal-Eh, Igor O. Lutsik, Ruslan Irkimbekov, Faezeh Rahmani, Hector R. Vega-Carrillo, *Nedis-Serpent simulation of a neutron source assembly with complex internal heterogeneous structure*, Applied Radiation and Isotopes, Volume 160, 2020, 109066, ISSN 0969-8043, https://doi.org/10.1016/j.apradiso.2020.109066.

[33] Lorenzi, S., Presentation for the course Experimental Nuclear Reactor Kinetics: TRIGA Introduction. Politecnico di Milano. Milano. 2021.

[34] Westinghouse Electric Corporatin, "Fission Counter," 86-284T datasheet, Nov. 1975.

[35] Westinghouse Electric Corporatin, "Uncompensated Triaxial Ionization Chamber System," 86-294T datasheet, Jun. 1976.

[36] Ghezzi, Carlotta Giuliana. *Development and Validation of a New Neutronic Model of the TRIGA Mark II Reactor.* Diploma Thesis. Milano. Politecnico di Milano, Department of Energy. 2019. Supervisor Prof. Antonio Cammi.

[37] Chiesa, Davide. *Development and Experimental Validation of a Monte Carlo Simulation Model for the TRIGA Mark II Reactor.* Ph.D. Thesis. Milano. University of Milano-Bicocca, Department of Physics. 2013. Supervisor Prof. Ezio Previtali.

[38] Gallego, Eduardo & Hernandez-Davila, Víctor & Lorente, Alfredo & Acuña, Enma & Sánchez, G. & Vega-Carrillo, Hector. (2005). Características dosimétricas de fuentes isotópicas de neutrones [Dosimetry Characteristics of the Isotopic Neutron Sources]. Revista Mexicana de Física. 51.

[39] LENA Applied Nuclear Energy Laboratory, "Regulation Control Rod Worth," datasheet, May 2015.

[40] Rataj, Jan, Ondřej Huml a Ľubomír Sklenka. Experimentální neutronová a reaktorová fyzika: laboratorní cvičení [Experimental Neutron and Reactor Physics]. Prague: Czech Technical University of Prague, Faculty of Nuclear Sciences and Physical Engineering, 2016. ISBN 978-80-01-05904-3.

[41] Biswal, A. (2022, August 11). Recurrent neural network (RNN) tutorial: Types and examples [updated]: Simplilearn. Simplilearn.com. Retrieved October 15, 2022, from https://www.simplilearn.com/tutorials/deep-learning-tutorial/rnn

[42] R. Dey and F. M. Salem, "Gate-variants of Gated Recurrent Unit (GRU) neural networks," 2017 IEEE 60th International Midwest Symposium on Circuits and Systems (MWSCAS), 2017, pp. 1597-1600, doi: 10.1109/MWSCAS.2017.8053243.

[43] Di Maio, F., Presentation for the course Integrated Deterministic and Probabilistic Safety Analysis of Nuclear Power Plants: Lecture 4d. Politecnico di Milano. Milano. 2021.

[44] Sharma, Siddharth, S Sharma and Anidhya Athaiya. Activation Functions in Neural Networks. Published Online April 2020 in International Journal of Engineering Applied Sciences and Technology, 2020 Vol. 4, Issue 12, ISSN No. 2455-2143, Pages 310-316. DOI:10.33564/ijeast.2020.v04i12.054

[45] HUML, Ondřej. *Neutronově fyzikální charakteristiky AZ C18 školního reaktoru VR-1* [*Neutron and Physical Characteristics of the core C18 of the school reactor VR-1*]. Prague. Czech Technical University of Prague, Faculty of Nuclear Sciences and Physical Engineering, Department of Nuclear Reactors.. 2020.

[46] Team, K. (n.d.). Keras documentation: About keras. Keras. Retrieved November 26, 2022, from https://keras.io/about/

Appendix A

Delayed neutron parameters of the TRIGA Mark II Pavia reactor

Table A.1: Delayed neutron parameters from forward delayed neutron parameters analogue estimator in Serpent2 for TRIGA Mark II Pavia reactor, nuclear data library ENDF/B-VIII.0

Group of DN	1	2	3	4	5	6
$\beta_{eff,i}$	2.2941E-04	1.1869E-03	1.1256E-03	2.5176E-03	1.0404E-03	4.3460E-04
λ_i	1.3336E-02	3.2693E-02	1.2068E-01	3.0285E-01	8.5046E-01	2.8544E+00

Appendix B

Emission spectra of AmBe and RaBe neutron sources

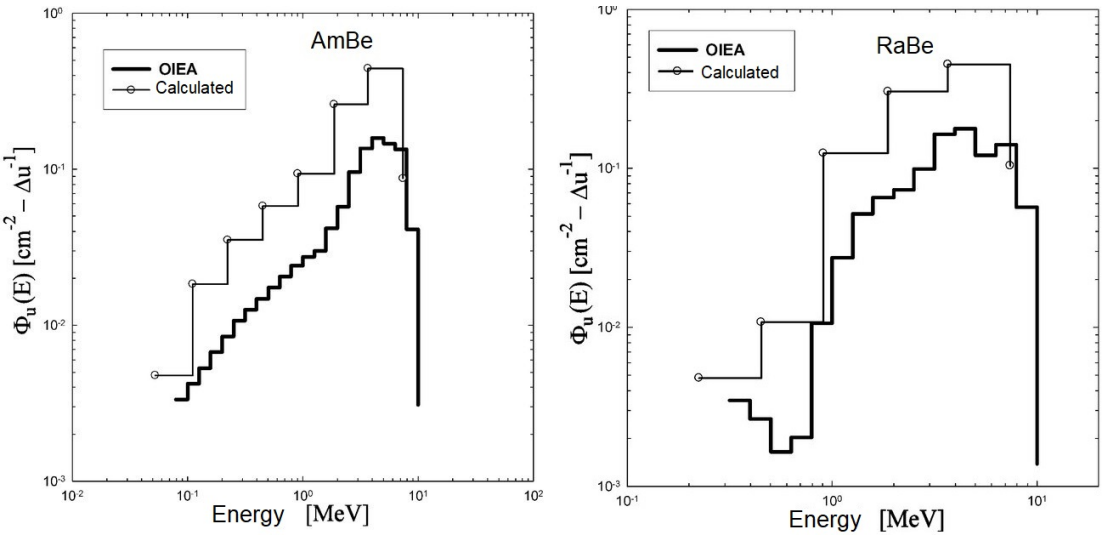

Figure B.1: Emission spectra of AmBe (left) and RaBe (right) neutron sources [38]

Appendix C

Code of the ANN in Python and its description

The code of the ANN is presented here together with its description.

```
pip install TensorFlow
## Loading the data with reactivity
from pathlib import Path
from os import listdir
from os.path import isfile, join
import numpy as np
import pandas as pd
import tensorflow as tf
from tensorflow import keras
from tensorflow.keras import layers
import matplotlib.pyplot as plt

path = r"pathtofiles"
only_files = [f for f in listdir(path) if isfile(join(path, f))]
data = []
for file_name in only_files:
    file_path = Path(path) / file_name
    print(file_path) # note: 6.1 and 22.1 are not included, I can
        include them if I want, need to calculate it in script6C18
    data.append(np.loadtxt(file_path, dtype = float))

## Definition of the variables
def variable_definition(data, column):
    list = []
    for i in range(len(data)):
        list.append(data[i][:,column])
    return list

pmv1 = variable_definition(data, 1)
pmv2 = variable_definition(data, 2)
pmv3 = variable_definition(data, 3)
pmv4 = variable_definition(data, 4)
rho = variable_definition(data, 11)

## Normalization of the data in the interval [0:1]
```

```
35
36 #Finding the maximum
37 def find_list_max(list):
38     max_value_list = list[0][0]
39     for i in range(len(list)):
40         for k in range(len(list[i])):
41             if np.all(list[i][k] > max_value_list):
42                 max_value_list = list[i][k]
43     return max_value_list
44
45 max_pmv1_value = find_list_max(pmv1)
46 max_pmv2_value = find_list_max(pmv2)
47 max_pmv3_value = find_list_max(pmv3)
48 max_pmv4_value = find_list_max(pmv4)
49
50 #Finding the minimum
51 def find_list_min(list):
52     min_value_list = list[0][0]
53     for i in range(len(list)):
54         for k in range(len(list[i])):
55             if np.all(list[i][k] < min_value_list):
56                 min_value_list = list[i][k]
57     return min_value_list
58
59 min_pmv1_value = find_list_min(pmv1)
60 min_pmv2_value = find_list_min(pmv2)
61 min_pmv3_value = find_list_min(pmv3)
62 min_pmv4_value = find_list_min(pmv4)
63
64 #Normalaziation
65 def normalise(list, max_value, min_value):
66     list_norm = []
67     list_nor = []
68     for j in range(len(list)):
69         for l in range(len(list[j])):
70             list_nor.append((list[j][l] - min_value)/(max_value -
                min_value))
71     list_norm = np.array(list_nor)
72     return list_norm
73
74 pmv1_norm = normalise(pmv1, max_pmv1_value, min_pmv1_value)
75 pmv2_norm = normalise(pmv2, max_pmv2_value, min_pmv2_value)
76 pmv3_norm = normalise(pmv3, max_pmv3_value, min_pmv3_value)
77 pmv4_norm = normalise(pmv4, max_pmv4_value, min_pmv4_value)
78
79 rho_nor = []
80 rho_norm = [] #rho is normalized only by a difference of 0.01 to get
    into the in interval [0:1]
81 for j in range(len(rho)):
82     for l in range(len(rho[j])):
83         rho_nor.append(rho[j][l]-0.01)
84 rho_norm = np.array(rho_nor)
85
86 ## Definition of the testing and training data,
87 train_size = int(0.70*len(pmv1_norm))
88 test_size = len(pmv1_norm) - train_size
```

```
89
90  train_set = [pmv1_norm[0:train_size],pmv2_norm[0:train_size],pmv3_norm
        [0:train_size],pmv4_norm[0:train_size],rho_norm[0:train_size]]
91  x_train_array = [train_set[0],train_set[1],train_set[2],train_set[3]]
92  x_train_trans = np.transpose(x_train_array)
93  x_train = tf.convert_to_tensor(x_train_trans) #converting the array
        into the tensor
94  x_train = np.reshape(x_train, (x_train.shape[0],1,x_train.shape[1]))
95  y_train_array = [train_set[4]]
96  y_train_trans = np.transpose(y_train_array)
97  y_train = tf.convert_to_tensor(y_train_trans)
98  print("x_train shape is", x_train.shape)
99  print("y_train shape is", y_train.shape)
100
101 test_set = [pmv1_norm[train_size:],pmv2_norm[train_size:],pmv3_norm[
        train_size:],pmv4_norm[train_size:],rho_norm[train_size:]]
102 x_test_array = [test_set[0],test_set[1],test_set[2],test_set[3]]
103 x_test_trans = np.transpose(x_test_array)
104 x_test = tf.convert_to_tensor(x_test_trans)
105 x_test = np.reshape(x_test, (x_test.shape[0],1,x_test.shape[1]))
106 y_test_array = [test_set[4]]
107 y_test_trans = np.transpose(y_test_array)
108 y_test = tf.convert_to_tensor(y_test_trans)
109
110 ##Creating the RNN ANN
111 input_size = 4 #four input features -> pmv1-4
112 seq_len = len(x_train) #number of time steps
113 inp_cell_size = 256 #Size of the hidden cell in the first layer
114
115 model = keras.models.Sequential()
116 model.add(layers.GRU(units=inp_cell_size, input_shape = (1, input_size)
        , activation = 'tanh',return_sequences = False))
117 model.add(layers.Dense(units=1,activation = 'sigmoid')) # number 1
        stands for 1 output of the dense layer - reactivity
118
119 print(model.summary())
120
121 #Defining loss, optimiser and metrics functions
122 loss_func = tf.keras.losses.MeanSquaredError(reduction="auto", name="
        mean_squared_error")
123 opt_func = tf.keras.optimizers.Adam(learning_rate=0.01)
124 metr_func = tf.keras.metrics.MeanAbsoluteError(name="
        mean_absolute_percentage_error")
125 #Compiling the model
126 model.compile(loss = loss_func, optimizer = opt_func, metrics =
        metr_func)
127
128 ##Training
129 epoc = 200
130 training = model.fit(x_train, y_train, epochs = epoc, shuffle = False,
        verbose = 2,validation_split = 0.17)
131
132 ## Plotting the loss function
133 plt.plot(training.history['loss'], label = "mean squared error")
134 plt.xlabel('Epochs')
135 plt.ylabel('Mean squared error')
```

```
136 plt.legend()
137 plt.show()
138
139 ## Prediction
140 y_pred = model.predict(x_test)
141 y_pred_inv = y_pred + 0.01
142 y_test_inv = y_test + 0.01
143
144 ## Graph of the prediction and test
145 plt.plot(y_pred_inv, label = "keff predicted")
146 plt.plot(y_test_inv, label = "keff from polynomial based on Serpent2
    calculation")
147 plt.xlabel('Time [0.1 s]')
148 plt.ylabel('k_eff')
149 plt.legend()
150 plt.show()
151
152 ## Saving the model architecture, weights, training configuration,
    state of the optimizer
153 import os.path
154 if os.path.isfile(r"pathtomodel.h5") is False:
155     model.save(r"pathtomodel.h5")
```

Firstly, TensorFlow must be installed, then on lines 3-11, the libraries used in the code are imported. On lines 13-19, the files from the directory `pathtofiles` are loaded and on lines 21-32 the variables must be defined. Then the minimum and the maximum of each variable is found on lines 36-62. Note that Python libraries and their functions can be used to find the minimum and maximum of the functions.

Data are normalized into the interval [0,1] on lines 65-84. Importantly, on line 71, all data from separate files are merged into one large vector that represents the time-series behaviour, similarly the same is done on line 84 for k_{eff} because the normalization for it is different. Note that k_{eff} is actually called rho in the code and its normalization is realised only by subtraction of 0.01. The values of k_{eff} should be in interval [0,1], but some critical or near-critical states were calculated as a value slightly higher than one. The data are still called normalised in order to keep logic of the next steps.

Testing and training data are defined on lines 87-108. Firstly 70 % of all data is defined as the training, then the train set is created, and importantly, must be converted into the tensor for the steps of ANN model creation. Similarly the test set is created. Then the ANN model itself is created from line 111. Firstly a number of inputs is defined (4 in case of 4 detectors), model layers are defined on lines 115-117. The batch size was remained as default, that is 32. Dense layer is the output layer of the ANN.

Further, the loss, optimiser and metrics functions are defined. Adam optimiser is a stochastic gradient descent method. A metric is a function that is used to judge the performance of the model. Metric functions are similar to loss functions, except that the results from evaluating a metric are not used when training the model.

The model must be compiled before the training. On line 129, a number of epochs to train the model is defined. An epoch is an iteration over the entire x and y data

provided and this particular model actually converged after about 100 epochs. The training defined on line 130 has an important parameter shuffle that must be set to `False`. If not, the time-series data would be shuffled and sequence of them would be violated. Lastly, the parameter `validation_split` defines the percentage of the training data used for testing. It is 17 % of the training data that fits more or less the 10 % of all the data used for validation.

Once the training phase is finished, it is a good practice to plot the loss function which is performed on lines 134-137.

To evaluate the performance of the model, a prediction must be done, such as on line 140, then the data must be denormalized which in this case was only by summing the constant of 0.01.

Finally, the prediction graph is generated on lines 145-150. The plot of k_{eff} predicted and k_{eff} from the polynomial is shown in Fig.: C.1. Afterwards, saving the model architecture, weights, training configuration and state of optimizer is performed. Once the model is saved, it only needs to be loaded and the desired data can be fed into the model to get the prediction.

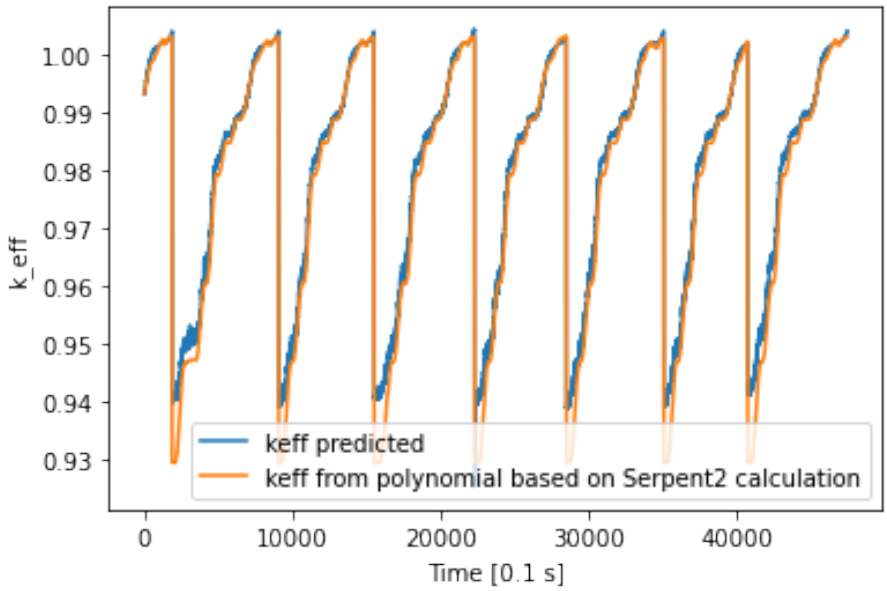

Figure C.1: A prediction of k_{eff} by ANN and by the polynomial based on Serpent2

It can be observed that the ANN was unable to predict reactivites in the deepest subcritical states (k_{eff} lower than 0.94). That is why, another approaches for the training where chosen, for instance a vector of zeros inserted in between every start-up data, so that the Recurrent Neural Network in the deepest subcritical states does not work with the data from the previous start-up (corresponding to the peaks in Fig.: C.1 where the critical states where reached). Nevertheless these approaches did not bring any other improvement.

Appendix D

Code in Python for online reactivity prediction by ANN and its description

The following code is prepared for the purposes of online reactivity prediction by ANN when loading the data in `.csv` file. The code is described and can be adjusted by small changes for each ANN training. This code can serve for online reactivity monitoring of any reactor for which the ANN was trained and tested. It only requires the data to be collected in `.csv` file and the parameter of β_{eff} for the given core to be defined. Lastly, the maximum values of the detector response observed in the training must be added into the code.

```
1  import tensorflow as tf
2  from tensorflow.keras.models import load_model
3  import numpy as np
4  import pandas as pd
5  import matplotlib.pyplot as plt
6  from matplotlib.pyplot import figure
7
8  ##Loading model
9  loaded_model = load_model(r"pathtomodel.h5")
10
11 def normalise(list, max_value, min_value):
12     list_norm = []
13     list_nor = []
14     for j in range(len(list)):
15         list_nor.append((list.iloc[j]- min_value)/(max_value -min_value
               ))
16     list_norm = np.array(list_nor)
17     return list_norm
18 ##Normalization of the data in the interval [0:1], Data must be
       normalized in the same interval as during the training!
19 #Using the maximum from the training part
20 max_pmv1_value = #Insert the maximum value of PMV1 from ANN training
21 max_pmv2_value = #Insert the maximum value of PMV2 from ANN training
22 max_pmv3_value = #Insert the maximum value of PMV3 from ANN training
23 max_pmv4_value = #Insert the maximum value of PMV4 from ANN training
24
```

```
25 #Using the minimum from the training part
26 min_pmv1_value = 0
27 min_pmv2_value = 0
28 min_pmv3_value = 0
29 min_pmv4_value = 0
30
31 #Loading csv
32 chunksize = 10
33 for chunk in pd.read_csv('pathtocsv.csv', chunksize=chunksize, header
       =0,encoding='latin-1', sep=';', usecols = ["N_PMV1_am","N_PMV2_am",
       "N_PMV3_am","N_PMV4_am"],dtype =np.float64):
34     pmv_all = chunk.iloc[:,0:4]
35
36     #Normalaziation
37     pmv1_norm = normalise(pmv_all.N_PMV1_am, max_pmv1_value,
           min_pmv1_value)
38     pmv2_norm = normalise(pmv_all.N_PMV2_am, max_pmv2_value,
           min_pmv2_value)
39     pmv3_norm = normalise(pmv_all.N_PMV3_am, max_pmv3_value,
           min_pmv3_value)
40     pmv4_norm = normalise(pmv_all.N_PMV4_am, max_pmv4_value,
           min_pmv4_value)
41
42     # Creating the test set to be predicted
43     test_set_array = [pmv1_norm,pmv2_norm,pmv3_norm,pmv4_norm]
44     test_set_trans = np.transpose(test_set_array)
45     test_set = tf.convert_to_tensor(test_set_trans)
46     test_set = np.reshape(test_set, (test_set.shape[0],1,test_set.shape
           [1]))
47
48     #Prediction
49     beta_eff = #Insert the value of beta_eff
50     keff_pred = loaded_model.predict(test_set)
51     keff_pred_inv = keff_pred + 0.01 #must be denormalised because it
           is already normalized by -0.01 in the loaded model
52     rho_pred = (keff_pred_inv -1)/(keff_pred_inv*beta_eff)
53     print("Reactivity predicted by ANN in $:",rho_pred)
54
55     #Plotting the prediction
56     plt.plot(rho_pred)
57     plt.xlabel('Time [0.1 s]',fontsize=18)
58     plt.xticks(fontsize=14)
59     plt.ylabel("rho predicted [\$]",fontsize=18)
60     plt.yticks(fontsize=14)
61     plt.show()
```

Firstly some used libraries are imported, then on line 9, the trained model is loaded. The path `pathtomodel` must be the same as for the saved model in the Appendix C.

Additionally, the normalization function is defined. Note that `.iloc[]` must have been added behind the list as the code works with pandas DataFrame further. It is important to normalize the count rates in the same interval as during the ANN training. Maximum values can be manually inserted from the code in Appendix C. The minimum value in case of VR-1 will always be zero, in other reactors the

minimum value could also be inserted.

Then a continuous `for` loop is defined for the online reactivity monitoring. On line 33, the `.csv` file is loaded. A chunk is used for reading large data files and its main advantage is that it can be used for online `.csv` file reading as it only loads the data in the so called chunks. `chunksize` must be defined by the user, it is a number of values that will be loaded. If the `chunksize` is 10, in case of VR-1 reactor, the data will be loaded every 1 second (given by 0.1 second time intervals for data collection). In the function argument on line 33, `pathtocsv` must be defined, then the names of the columns are defined, e.g. in VR-1 reactor, a column containing detector count rates from PMV1 is called `N_PMV1_am`.

Once the data are loaded, they are normalized on lines 37-40 by the pre-defined function. Afterwards, the test set from the chunk is created similarly as in code in Appendix C. In case the `chunksize` is 10, a test set of 10 lines is created.

Finally, the prediction based on the `loaded_model` of the created `test_set` is done on line 50. Then the data are inverted (or denormalised) as the normalisation is already performed in the previous code. Data are converted from k_{eff} into ρ on line 52, this step requires β_{eff} to be defined on line 49. Finally, the value of reactivity is printed on line 53. Then, depending on the user, the reactivity values can also be printed in the graph, which is performed on lines 56-61.